Document Title: A Statistical Validation of the Individuality of Guns Using High Resolution Topographical Images of Bullets

Author: Intelligent Automation, Inc.

Document No.: 232136

Date Received: October 2010

Award Number: 2006-DN-BX-K030

A Statistical Validation of the Individuality of Guns Using High Resolution Topographical Images of Bullets

Grant Number: 2006-DN-BX-K030

Final Report

Period Covered: August 01, 2006 – April 30, 2007

Submitted by:

Intelligent Automation, Inc.
15400 Calhoun Drive, Suite 400
Rockville, MD 20855

This project was supported under award number 2006-DN-BX-K030 from the National Institute of Justice Office of Justice Programs, U.S. Department of Justice. Points of view in this document are those of the author(s) and do not necessarily represent the official position of the U.S. Department of Justice.

1. Table of Contents

2. Abstract

The ability to validate that an evidence bullet was fired by a suspect weapon can be of significant importance during the presentation of a case in court. The admissibility of firearms evidence rarely meets significant challenges. However, Supreme Court decisions such as Daubert and Kumho are making it increasingly necessary to further formalize scientific evidence presented in court. Thanks to the support of the National Institute of Justice (NIJ), in 2005 Intelligent Automation Inc. (IAI) completed a study named "A Statistical Validation of the Individuality of Guns Using 3D Images of Bullets". The objective of the 2005 NIJ Study was to validate the premise that the features transferred from a barrel to a bullet are sufficiently unique to allow for a one-to-one association between the barrel and the bullets. As part of this study, over 2800 bullets were fired, retrieved and compared using an automated ballistic analysis system developed by IAI for this study. A key element of innovation in that study was the development of a topography-based (or 3D based) automated system. Such system had never been developed before. The statistical analysis of the results of the comparisons performed by the automated system demonstrates that the premise of firearms identification can be validated in a quantitative manner. However, although very satisfactory for barrels of typical manufacture quality, the results of that analysis were less adequate in the case of both very poor and very good quality barrels. Furthermore, these deficiencies were magnified when damaged bullets were considered.

The main goals of the present study were to extend the results obtained in our previous effort to barrels of very poor and very good manufacture quality for both pristine and damaged bullets. At the completion of this study we conclude that the trueness of the premise of firearms identification can be extended to the majority of such barrels. Among the barrel brands used in this study, the notable exception was those of Bryco manufacture. In the case of such barrels, the variability found on bullets fired by the same barrel was so extreme, that the feasibility of a reliable identification appears questionable. Having made such statement, we must caveat it with another important conclusion of the present study; which is that the ability to determine that a given bullet was fired by a specific barrel depends on the individual barrel itself and not only on the brand of its manufacture. In addition, it is important to emphasize that the performance of the automated analysis system used in this study is not representative of that of a trained firearms examiner.

3. Executive Summary

3.1 Introduction

Weapon identification, its procedures and methodologies, have been developed over the past 100 years. These procedures are routinely used by firearms examiners and are the basis of their testimony in court. As currently practiced, these procedures involve a firearms examiner looking at the surface of bullets and attempting to determine whether they were fired by the same gun. In reaching such conclusions, the firearms examiner relies mostly on his/her training, judgment and experience, making current matching procedures mostly subjective. The development of DNA identification techniques and the level of accuracy achievable in the estimation of error rates associated with DNA identification has raised the expectations of the quantitative precision that may be achieved in forensic analysis. Furthermore, recent Supreme Court decisions such as Daubert [1] and Kumho [2] are making it increasingly necessary to further formalize the presentation of scientific evidence in court. The subjective nature of current identification criteria, together with the inability of existing matching methodologies to estimate the probability of error associated with identification may pose a serious problem for the use of firearms evidence in court.

Intelligent Automation Inc. has conducted a variety of studies on the validation of the individuality of guns using topographical images of bullets. These studies had in common the fact that topographical images (as opposed to photographical images) were used to perform comparisons of the Land Engraved Areas (LEAs). The largest such study was conducted thanks to the support of the National Institute of Justice (NIJ) and it was completed in 2005 [4]. While the results of the 2005 NIJ Study were very satisfactory for barrels of typical manufacture quality (in the sense of validating the basic premises of ballistic evidence identification), they were less persuasive in the case of both very poor and very high quality barrels (where in the context of this study the “quality” of a barrel pertains exclusively to the manner in which features are transferred between the barrel and the bullets fired by it). These deficiencies were further magnified when damaged bullets were considered. Some of the key factors responsible for the limitations of the results observed in the 2005 NIJ Study were identified prior to the present study. For example, barrels of poor quality are often manufactured with an oversized bore. The over-sizing of the bore results in poor transference of features between the barrel and the bullets. At the other end of the spectrum are barrels of very good manufacture quality. The rifling of these barrels is often polished to such an extent that the features transferred to the bullet have very little depth, making their detection challenging for most instruments. The inability to demonstrate the premise of firearms identification in a quantitative manner for these barrels poses a threat to the future admissibility of this evidence in court.

The factors associated with the limitations of the 2005 NIJ Study can be classified as hardware-related and algorithmic-related. Figure 1 shows the data acquisition system used in the 2005 NIJ Study. While this instrumentation was state-of-the-art at the inception of the study, and it provided an excellent platform for the majority of bullets/barrels for which it was used, it has become evident that the depth resolution of the sensor at the core of this system was not sufficient for the acquisition of features found on bullets fired by very high quality barrels (by very high quality we mean those barrels which rifling finish is significantly above average). The reason for such deficiency is that the interior of such barrels is polished to such a degree during manufacture, that the features transferred between the barrel and a bullet are very shallow, and tend to be overcome by the instrument's noise. It should be noted that prior to the completion of our study, there was no knowledge regarding the depth resolution required to obtain individual data from the surface of bullets.

Figure 1: Data Acquisition System used in 2005 NIJ study

Another important limitation of the hardware used in the previous project was the achievable speed of data acquisition. Due to the limited acquisition speed, it was not practical to acquire all data necessary to fully characterize the LEAs of the bullets under analysis. This limitation did not present a problem in the case of LEAs presenting clear, well defined striations (because in such cases the assumption that most of the data found on a LEA is striated was satisfied), but it prevented the processing algorithms from correctly processing LEAs of unusual geometry such as those found on bullets fired by barrels of low quality. Figure 2 provides a graphic representation of this problem. The image shown in Figure 2 is a photo-realistic rendering of a single LEA as acquired by a white light confocal microscope used in the present study (the base of the bullet is at the bottom of the image). This data set is comprised of 470 cross sections (corresponding to horizontal lines), and is rich enough to allow for a realistic rendering of the LEA. By comparison, the data acquired by the data acquisition hardware used in the 2005 NIJ Study would have been limited to 5 cross sections only (such as shown by the red "horizontal" lines).

The richness of the 3D surface topography measured by the confocal microscope clearly shows that the striations found on a LEA may not extend over the entire width of the bullet's LEA. This phenomena is more prominent in the case of barrels of poor manufacture quality. LEA areas contain no striations are often referred to as "bad data regions" from the automated ballistic identification point of view. The data acquired by the data acquisition hardware used in the 2005 study was so sparse, that it prevented the identification of such bad data regions. The algorithms used in that study would have proceeded to use such data as if it were valid, resulting in the "contamination" of significant amounts of LEA data. Herein lays the algorithmic-related limitations of the 2005 Study. The imaging capability of the confocal microscope provides the

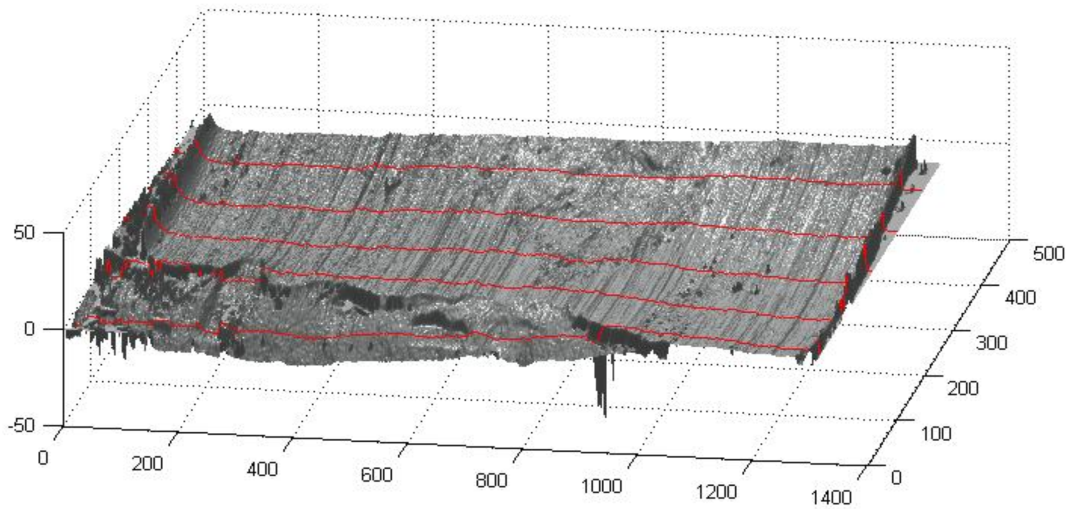

Figure 2: Comparison of data acquisition capabilities of single point vs. patch sensor. The single point sensor would have only acquired the data indicated by the red lines. The confocal microscope allows the acquisition of all the data shown in this image.

means to overcoming this limitation by either using automated pattern recognition techniques or by simply manually excluding those regions deemed to contain bad date.

In summary, while the results of the 2005 NIJ Study were very satisfactory for typical barrels, they were less satisfactory for barrels of very good or very poor quality. In order to extend these results, the present study makes use of new data acquisition hardware with high depth resolution and fast acquisition speed was used as part of the present study. The use of an instrument with enhanced depth resolution has produced significant improvement in the successful analysis of bullets fired by very good quality barrels. However, improved depth resolution by itself will not solve the challenges associated with bullets fired by barrels of poor quality. The successful analysis of such bullets requires the handling of regions of poor quality data (either automatically or manually).

3.2 Scope of the Study

Based on the above discussion, the main goals of the current study were the following:

a) To validate the premise that the features transferred between a barrel and a bullet are sufficiently unique to allow for a one-to-one association between bullet and barrel for barrels of very poor and very good quality.

b) To improve our understanding of the parameters associated with the individuality of the features transferred between a barrel and a bullet.

4. Technical Report

4.1 Project Design, Data and Methods

The approach followed in this study relied on three main elements: a) the use of topographical data (or 3D data) for the characterization of the surface of the bullets under analysis, b) the use of a consistent and objective processing of the data to develop a set of "signatures" for each of the bullets under analysis, and c) the use of well established statistical techniques to quantify the degree to which individual bullets can be associated as being fired by the same barrel.

- Measurement field: 800/320 micrometers.
- X/Y-Resolution: 1.5/0.6 micrometers.
- Z-Resolution: 20/10 nanometers.
- Numerical Aperture: 0.40/0.50.
- Working Distance: 12/10.6 mm

Figure 3: NanoFocus' White Light Confocal Microscope (MuSurf)

4.1.1 Topography-based Automated Ballistic Analysis System

The data acquisition system used in this study is a white light confocal microscope manufactured by NanoFocus AG. Figure 3 shows the microscope. While the instrumentation used in the 2005 Study could only acquire a single point at a time, this device is capable of acquiring patches of 512 by 512 points simultaneously in seconds and is capable of "stitching" multiple patches to create much larger data sets. Most importantly, this device offers a resolution of up to 10 nanometers in depth, which is significantly better than that of the equipment used in the 2005 study. The ability to acquire more and substantially better data is vital in our efforts to extend the results already obtained for typical barrels to barrels of very poor and very good quality. For each of the barrel brands under consideration, 10 barrels were selected (except in the case of Taurus, where only 6 barrels were available). 5 pristine bullets and 2 damaged bullets were selected for each of these barrels. A summary of the total amount of data used in this study, including the total number of LEAs acquired is shown in Table 1 below.

In order to systematically acquire bullets using the data acquisition hardware, a simple bullet

	Manufacturer	No. of Barrels	No. of Bullets per barrel	No. of Impressions per bullet	Total no. of Impressions per brand
1	Browning	10	7	6	420
2	Bryco	10	7	6	420
3	HiPoint	10	7	6 or 9	420 - 630
4	SIG	10	7	6	420
5	Taurus	6	7	6	252

Table 1: Summary of Data Sources Used in Study

positioning fixture was used (see Figure 4). This positioning fixture facilitates simple manipulation such as the rotation of the bullet surface and appropriate positioning of the bullet under the microscope lens to enable the easy acquisition of land impression data from the bullet surface. This positioning fixture is manually operated.

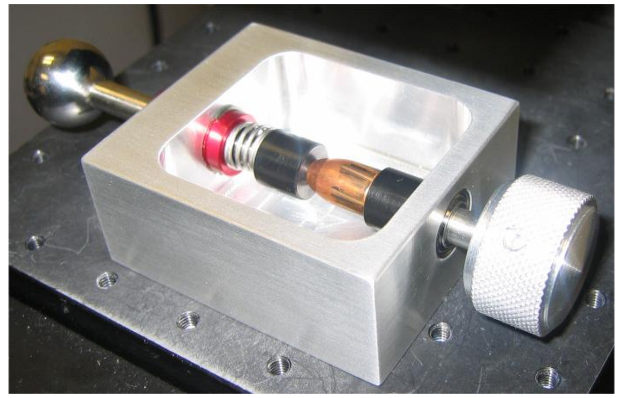

Figure 4: Bullet positioning fixture

The process of acquiring the land impressions from the bullets is as follows. The land impression on the bullet to be acquired is first identified. The bullet is then placed in the bullet positioning fixture under the confocal microscope and the bullet positioning fixture is manipulated such that the land impression of interest lies in the focal plane of the lens. Once the data acquisition parameters have been set with the help of the software application associated with the data acquisition hardware, the acquisition of the impression of interest begins. Figure 4 shows images of the bullet positioning fixture under the hardware system along with a close-up view of the bullet within the positioning fixture.

Upon the completion of data acquisition of one LEA, the knob on the bullet positioning fixture is used to position the next LEA of interest such in the field of view of the microscope. The data acquisition parameters are then set again based on the acquisition protocol, and the data acquisition is initiated. In this fashion, all the LEAs on a bullet are acquired by following the acquisition protocol. The topographical data acquired by the confocal microscope is then stored

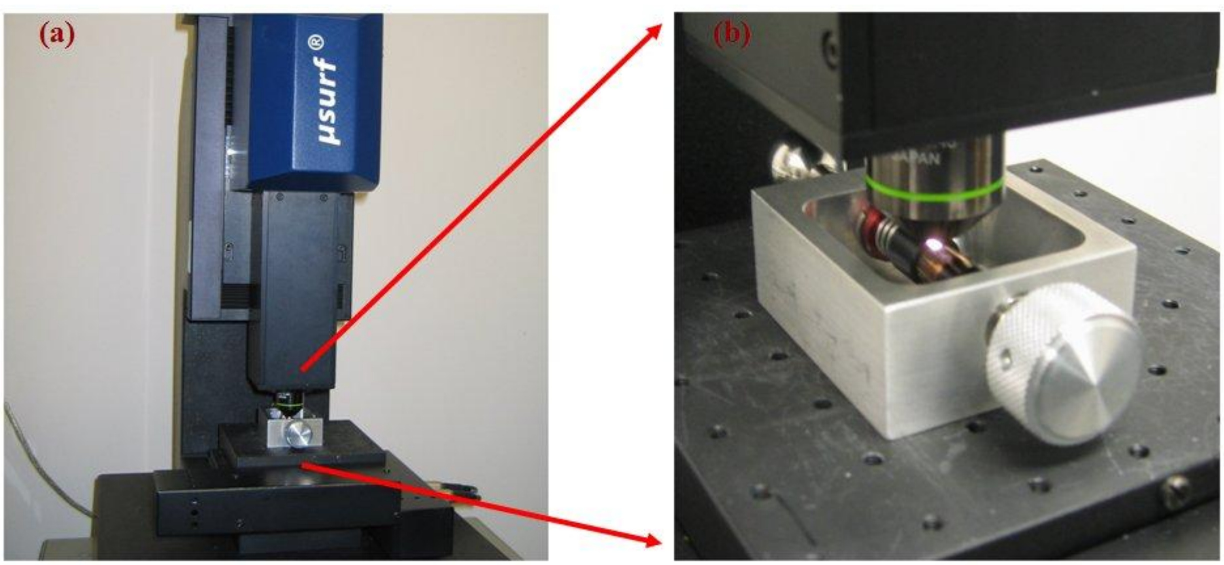

Figure 5: (a) Acquisition of topographical data of land impressions from the confocal microscope, and (b) close-up view of data being acquired from bullet placed in the positioning fixture.

in a database for subsequent analysis and processing.

Figure 6 shows pseudo-realistic representations (based on topographical data acquired as part of this study) of the six land impressions corresponding to a single bullet fired by a Browning barrel. These LEAs are organized top-to-bottom, starting from LEA 1 and ending in LEA 6 (i.e. going from top to bottom of Figure 6 corresponds to traveling along the base of the bullet clockwise). Notice the clear definition of the land impressions (or equivalently, the clear transition between land impression and groove impression). As expected, the widths of the LEAs found on this bullet are the same for all LEAs (consistent with a barrel rifled with grooves of equal width). Also, notice the presence of striated tool marks towards the base of the bullet, at the bottom of the land impressions. Notice too that a large proportion of the LEA includes "bad data regions" or regions where no striations are present. The images shown in Figure 6 are characteristic of very good quality barrel in the sense that the features transferred between the barrel and bullets, although faint, are very well defined and consistent along the different LEAs. The reason that the striations found in these bullets are faint is due to the careful polishing of the barrel as part of its manufacturing process.

By contrast, let us consider the features found on the surface of LEAs resulting from the firing of a bullet through a Bryco barrel. Figure 7 shows a pseudo-realistic rendering of the land impressions found on a bullet fired through a Bryco barrel. In many of these LEAs one cannot identify a clear transition between the land impressions and groove impressions (one

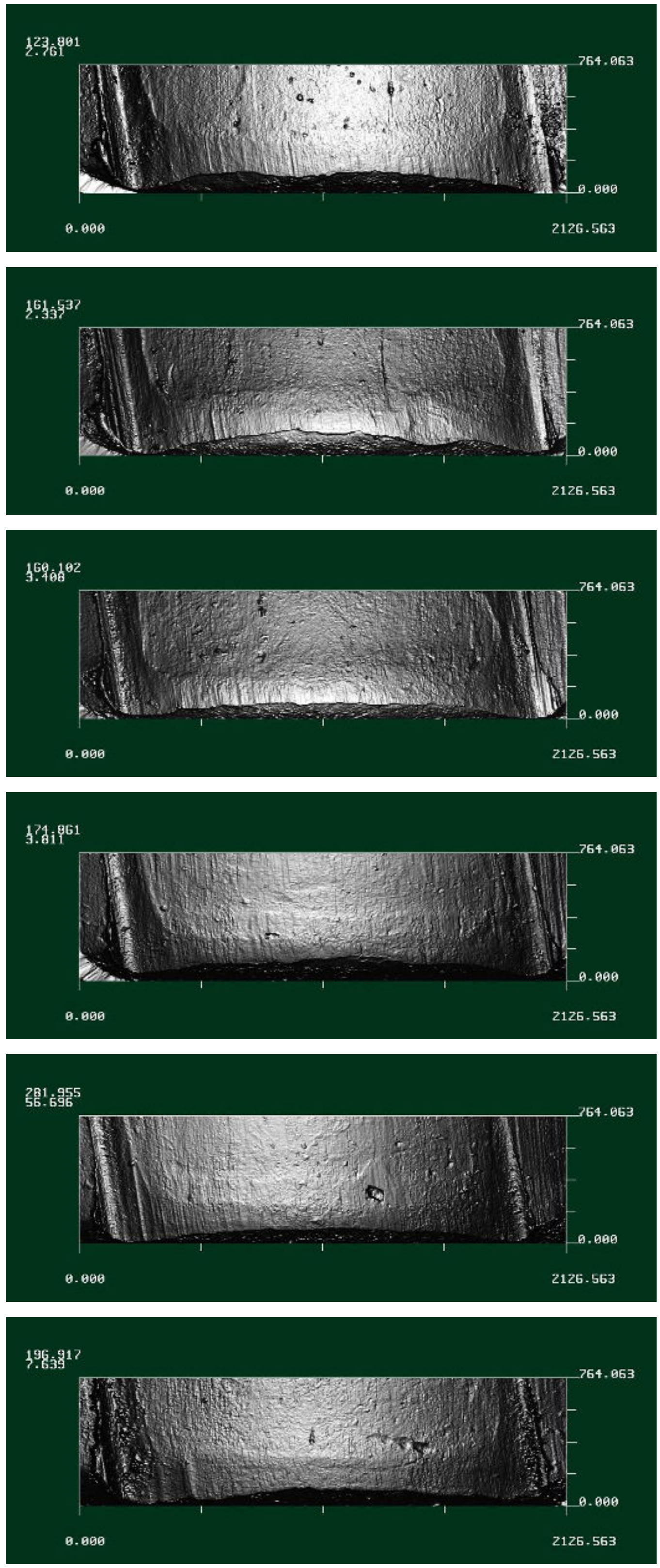

Figure 6: Photorealistic rendering of Browning LEAs 1 – 6 of barrel 6, bullet 2.

transition is often clearer than the other, due to the direction of rotation of the bullet inside the barrel). Moreover, the apparent width of these LEAs is very different from each other. This phenomenon is due to the fact that the surface of the bullets "slips" inside the barrel, and do not maintain a consistent contact with the barrel's interior surface. Notice also how LEA 1 (at the top of Figure 7) displays clear, deep striated tool marks (indicative of strong contact between the bullet and the barrel), while the rest of the LEAs display very few striated tool marks (indicative of weak contact between bullet and barrel).

The fact most of the LEAs make such weak contact with the barrel can be explained by an oversized barrel bore. While we did not engage in a systematic measurement of the bores of the different barrels considered in this study, we did see clear evidence of over sizing in the Bryco barrel's bores. In addition, as already mentioned, notice that one of the LEAs of the bullet imaged in Figure 7 made strong contact with the interior of the barrel (LEA 1, at the top) while the rest of them did not. This seems to indicate an uneven trajectory (and probably erratic) of the bullet inside the barrel (such that LEA 1 was pressed with greater force against the barrel than the rest of the LEAs). If the trajectory followed by the bullets fired by a given barrel is not consistent between different bullet firings, one should expect that the challenge of a successful identification will be compounded.

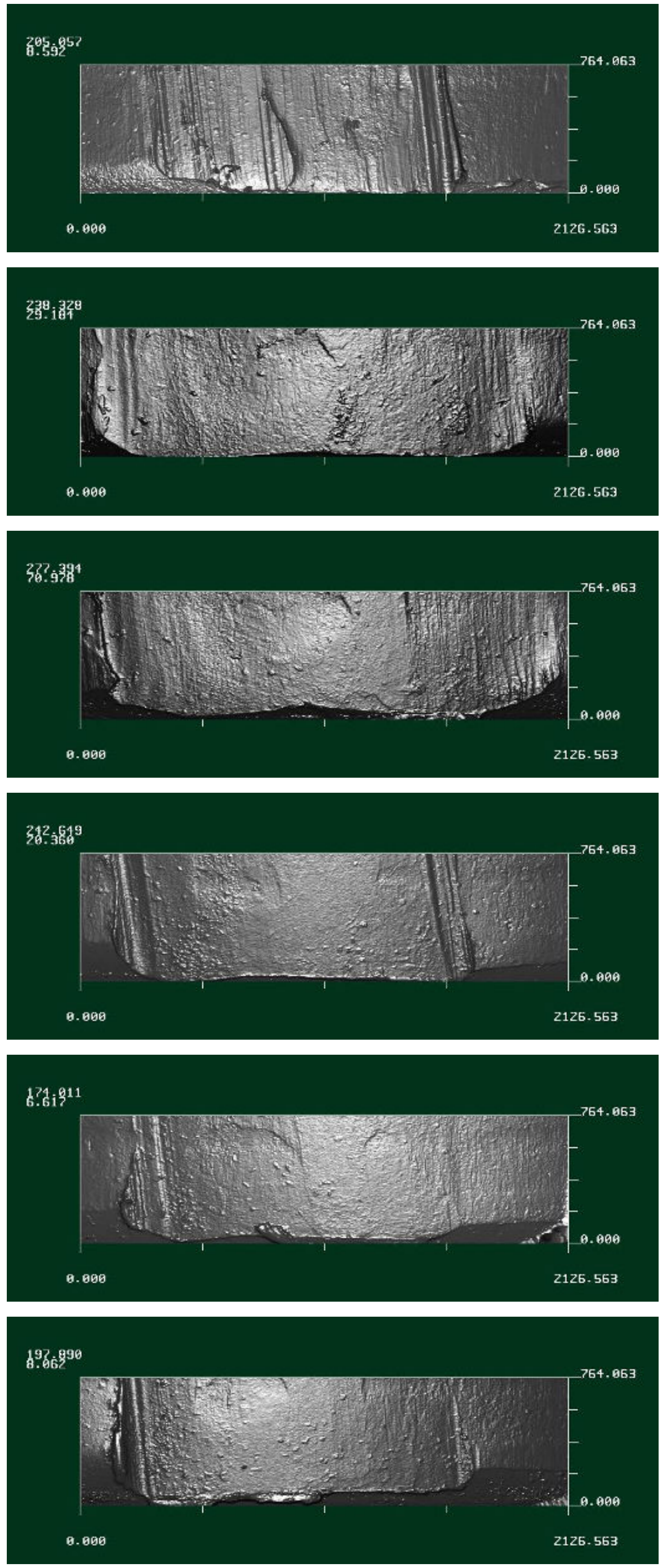

Figure 7: Photorealistic rendering of Bryco LEAs 1 – 6 of barrel 6, bullet 2.

4.1.2 Similarity Measure

We begin our discussion by reviewing the manner in which the similarity measure

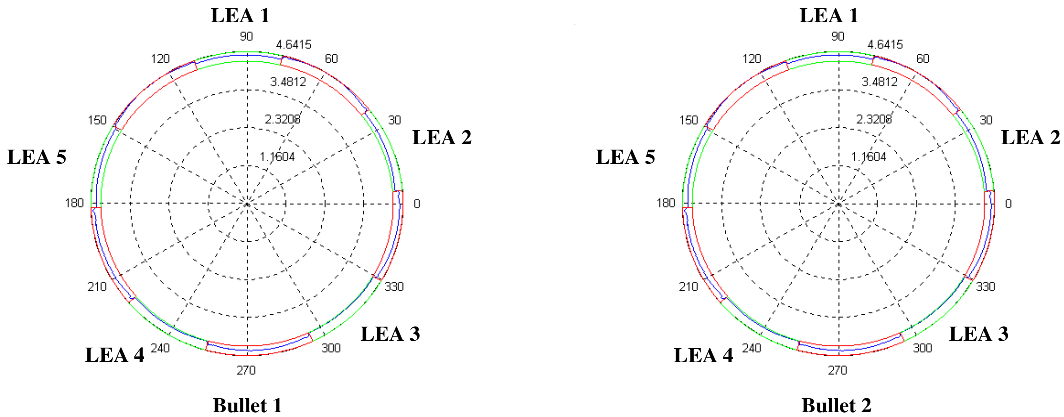

Figure 8: Relative Orientation between a Pair of Bullets

between two bullets is computed. Figure 8 shows an example of the cross-section of two bullets to be compared, each having 5 LEAs. In both of these cross sections, the LEAs have been labeled. From Figure 8 it should be clear that two bullets (with the same number of LEAs) can be compared in a number of relative "orientations". For example, one such orientation is consistent with comparing LEA 1 of bullet 1 with LEA 1 of bullet 2, LEA 2 of bullet 1 with LEA 2 of bullet 2, up to LEA 5 of bullet 1 with LEA 5 of bullet 2. This is in fact the orientation shown in Figure 1. However, if we "rotate" bullet 2 counter-clockwise by one LEA, the resulting relative orientation would be consistent with comparing LEA 1 of bullet 1 with LEA 2 of bullet 2, LEA 2 of bullet 1 with LEA 3 of bullet 2, up to LEA 5 of bullet 1 with LEA 1 of bullet 2. In other words, because the pair of bullets under consideration has five rifling impressions, they can be compared in five possible relative orientations. In general, a pair of bullets having *n* LEAs can be compared in *n* possible relative orientations.

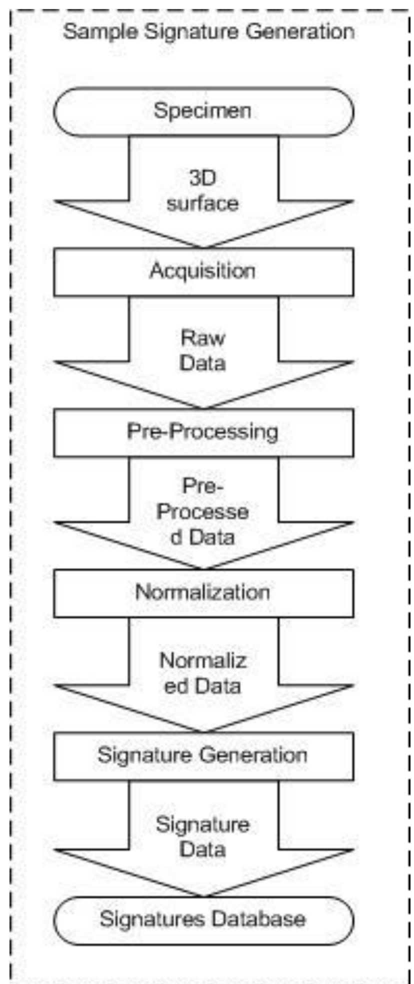

Figure 9: Signature generation processing pipeline

4.1.2.1 Bullet to Bullet Similarity Measure

The similarity measure between two bullets is computed by a) evaluating each possible LEA-to-LEA similarity b) selecting the orientation which is optimal in some pre-established sense and c) assigning a similarity measure to the optimal orientation based on the LEA-to-LEA similarity measures consistent with the optimal orientation. The final similarity measure for the bullet pair under comparison is given by this value.

The computation of the LEA-to-LEA similarity measure requires a sequence of steps. These steps include data pre-processing, normalization and signature generation. Figure 9 shows the main algorithmic components for generating the LEA signatures. The pre-processing is responsible for the identification and preliminary handling of unreliable data points (dropouts and outliers). The purpose of normalization is to “flatten out” the curved surface of the LEA in order to compensate for the curvature of all bullets of the same caliber (which is in fact a class characteristic). The normalization process is also designed to compensate for systematic errors during the acquisition process (such as variations in tilt during acquisition). After the normalization process, the signature generation is responsible for isolating the features that are unique to the LEA under consideration (individual features) while rejecting those features which are common to all LEAs of bullets of the same class (class characteristics). After band pass filtering, these normalized LEA cross section become the signatures of the bullet.

4.1.2.2 Pre-processing and Signature Generation (Fully Automated)

The purpose of the data pre-processing module is to identify and handle unreliable data points. These include dropouts (points that the imaging sensor was not able to acquire) and outliers (points that the imaging sensor managed to acquire, but which are inaccurate or noisy). For this reason, the data pre-processing module consists of a four step process: 1) identification of dropouts, 2) identification of outliers, 3) recording of both types of unreliable points, 4) isolation of region of interest, and 5) interpolation of the unreliable data. These steps are described below.

Identification of dropped points:

Most 3D imaging systems provide the user with a “level of confidence” value associated with each acquired data point (for optical systems, the level of confidence usually corresponds to the percentage of light reflected by the target). If said level of confidence is too low, the point is considered a dropout (i.e. it was “dropped” by the instrument) and is deemed “unreliable.”

Identification of outliers:

As opposed to dropped points, “outliers” are data points inaccurately measured by the 3D imaging system, which are not reported to the user as inaccurate by the acquisition hardware (via the level of confidence or reflectivity information). For this reason, they are much more challenging to identify. The approach used by our algorithms to detect outliers is by estimating the local slope between a point and its neighbors. If the slope is above a certain threshold, the point will be identified as an outlier.

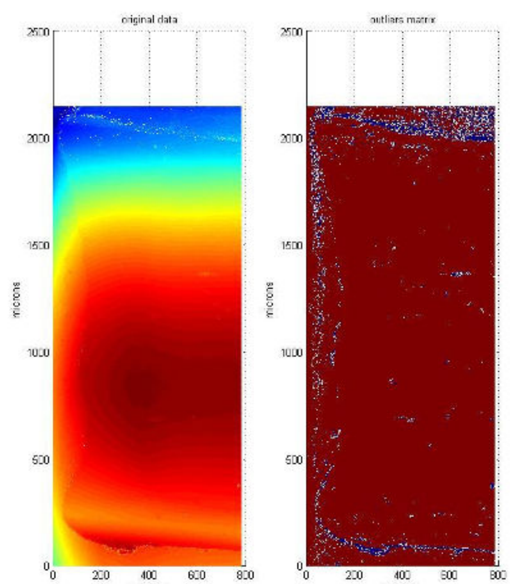

Figure 10: Outliers Identification

Recording of unreliable points:

Once all dropped and outlier points are identified, a "mask" is created to store this information for use during the comparison stages so that the unreliable points can be excluded from the comparison. In the current software implementation, the mask is an array of the same dimensions as the data, and its entries are "1' for those points deemed to be reliable, and "0" for those points identified as dropouts, outliers, or other unreliable, noisy points. The left side of Figure 10 shows an example of raw data, where the third dimension (*z*-axis) is color coded. The right side of Figure 10 shows the corresponding mask, where the points identified as dropouts or outliers have been colored blue, while the points deemed "reliable" have been colored red.

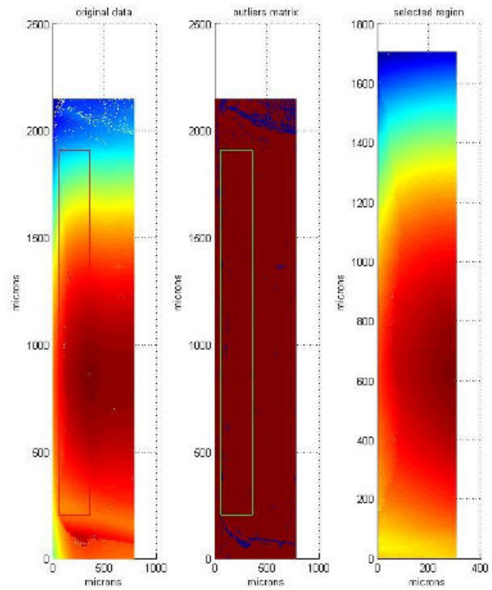

Figure 11: Automated Boundary Contraction

Isolation of Region of Interest:

Having identified points of questionable reliability, the current algorithms identify a "region of interest" over which to continue the analysis. This region of interest is meant to isolate the portion of the LEA which is most likely to contain the striated portion of the LEA. Figure 11 shows the effect of the algorithm developed for the purpose of isolating the regions of interest (or also called "boundary contraction") based on the data and mask shown in Figure 10. The left image in Figure 11 corresponds to the identification of the region of interest on the data; the center image shown in Figure 11 shows the same, but this time over the "mask". The right-most image in Figure 11 shows the data which has been selected as the region of greatest interest. Notice that the selected region of interest corresponds to the base of the LEA.

Interpolation:

For display purposes and in order to accommodate the digital filtering performed at a subsequent stage, the values of dropped points and outliers are replaced by interpolated values based on the neighboring points. Figure 12 shows the effect of the interpolation algorithm as applied to the

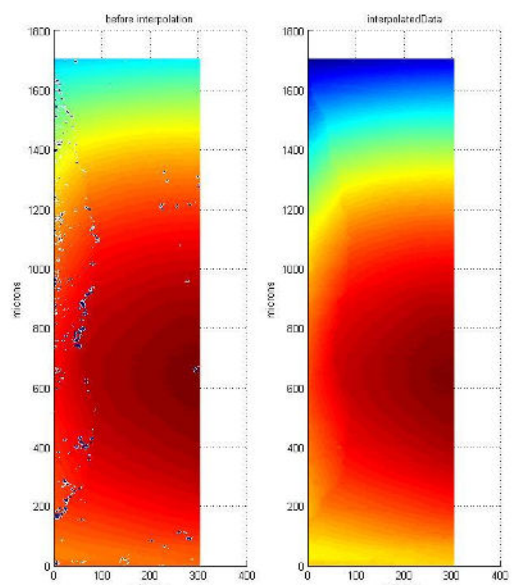

Figure 12: Interpolation

region of interest identified in the previous step. The left side of Figure 12 shows the data before interpolation (notice the “pockmarks” on the left side of the image, which correspond to unreliable data points); while the right side of Figure 12 shows the same data after unreliable points have been interpolated.

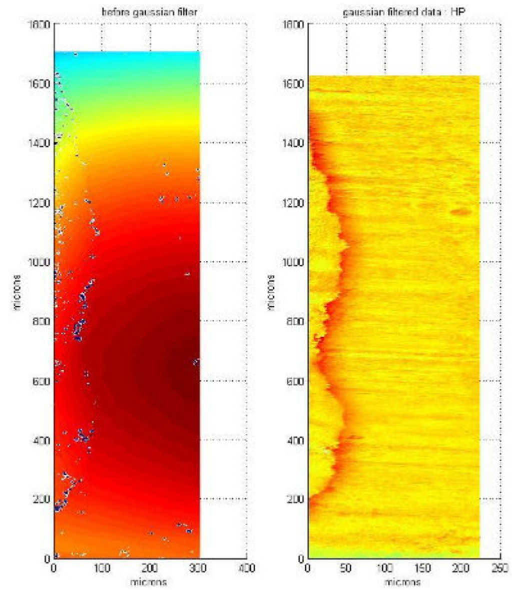

Figure 13: Gaussian HPF

High Pass Filtering:

The first step in the signature generation is the application of a high-pass Gussian filter to the interpolated data. The purpose of this step is primarily to reject the low frequency components associated with the curvature of the bullets, which amounts to a class characteristic and is therefore unsuitable for individual characterization. Figure 13 shows the effect of the application of the Gaussian filter. The left side of Figure 13 shows the identified region of interest, while the right side of Figure 13 shows the result of high pass filtering the interpolated data corresponding to the same region. As expected, the high pass filter emphasizes the high frequency content corresponding to the striations, while it rejects the low frequency content corresponding to the curvature of the bullet. While the striations are virtually invisible on the image on the left side of Figure 13 (due to the scale), they are very clear on the right side of Figure 13.

Identification of Rifling Angle

The next step associated with the generation of the LEA signature is the identification of the “lay orientation” or the orientation of the striations found on the LEA under analysis (this orientation angle is called the “rifling angle”). This step is necessary for two reasons: a) the orientation of the striations with respect to the base of a bullet differs from barrel brand to barrel brand. The rifling angle can be positive or negative (corresponding to “right” or “left” rifling), and it is normally between 7 and 10 degrees, b) since the topography of each LEA is acquired manually, there is always a small amount of variability in the resulting imaged data even with respect to the average rifling angle for the barrel brand under consideration. For this reason, the identification of the rifling angle is an

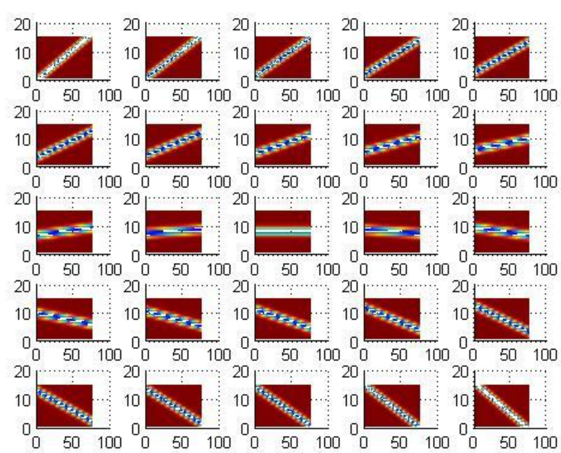

Figure 14: Striation Direction Filter Bank

important part of the analysis of each LEA.

In the fully automated version of the software developed for this project, the identification of the rifling angle is accomplished using a bank of filters similar to Gabor filters commonly used for identification of ridges in automated fingerprint comparison systems [5]. Figure 14 shows a bank of 25 different filters. These filters are variants of the same canonical filter, where each variant is a rotated version of the canonical filter. In this manner, each of these 25 filters is designed to evaluate the degree of similarity between the orientation of the filter and the striations found on the surface of the LEA. The bank of filters shown in Figure 14 is designed to identify striations at angles ranging from -12 degrees to +12 degrees (in 1 degree increments).

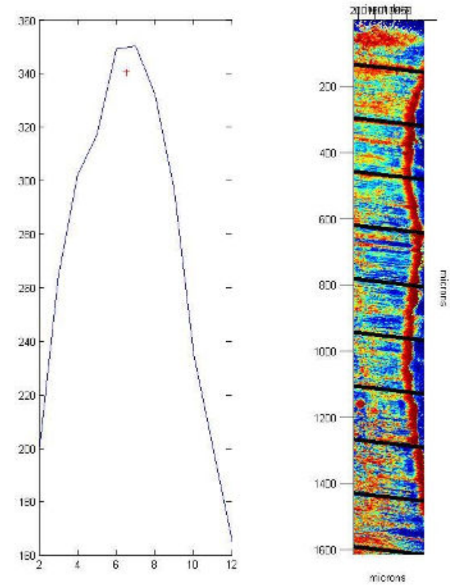

Figure 15: Automated Lay Direction Estimation

In order to identify the rifling angle, the high pass Gaussian filtered image of the LEA (see the image on the right side of Figure 13) is filtered by each of the different filters shown in Figure 14. As the filtering of the high pass Gaussian filtered image of the LEA by the filters shown in Figure 14 corresponds to a convolution function, the point-by-point value of the resulting filtered image provides a value approximately proportional to the degree of similarity between the features found on the high pass Gaussian filtered image of the LEA and the filter under consideration. The statistical properties of the filtered image, therefore, provide an indication of the degree of similarity between the features found on the high pass Gaussian filtered image and the angle of the filter applied to it (out of the 25 possible filters in the filter bank). The statistical value used to evaluate this similarity was the number of points in the post-filtered image that exceeded a given threshold.

The left side of Figure 15 shows a plot of the proposed statistic as a function of the orientation of the filters in the filter bank between 2 degrees and 12 degrees. This plot allows us to estimate the optimal estimate of the striations orientation (by seeking the maximum of the plot). The right side of Figure 15 shows 10 black parallel lines drawn at the estimated rifling angle superimposed over a LEA (to be precise, the parallel lines are superimposed over the LEA after it is histogram equalized). As can be seen, the resulting estimated striation angle (indicated by the black parallel lines superimposed on the histogram equalized LEA) is quite accurate. This method worked quite well for most LEAs in the study. The only instance where this approach did not perform well was when there were virtually no striations on the LEAs under analysis.

Profile Generation:

Once the orientation of the striations found on the LEA is identified, the high pass filtered LEA data can be "collapsed" along the direction of the striations. This process provides us with a "profile" of the LEA. It is worth noting that in the creation of this profile we exclude any points identified as unreliable during the initial steps of pre-processing. An example of such profile for the high pass filtered LEA shown in Figure 13 can be seen on the top part of Figure 16.

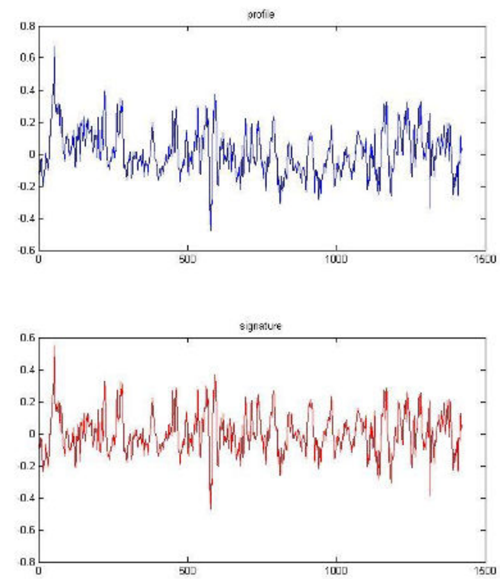

Figure 16: Profile and Signature Generation

Signature Generation:

The final step in the generation of a LEA signature is a high pass filtering of the LEA profile. This is a very low frequency high pass filter (in other words, it only filters out features of very high curvature). The purpose of this filter is to eliminate any remnant of the bullet surface curvature. The bottom image of Figure 16 shows the effect of applying this high pass filter to the profile data in the top of the same figure.

4.1.2.3 Pre-processing and Signature Generation (Partially Automated)

The algorithms described in Section 4.1.2.2 perform quite well for bullets whose LEAs displayed clear, well defined striations. However, even after considerable efforts, we were not able to develop algorithms sufficiently robust to perform well in the case of LEAs which did not display reasonably defined striations. This was the case of those bullets fired by barrels of poor quality. It is worth emphasizing that IAI spent considerable efforts developing algorithms of increased robustness. However, we did not succeed in the development of algorithms of sufficient robustness as to guarantee meaningful results for the objectives of this study. As an illustration, consider again the LEAs found on a bullet fired by Bryco barrel (see Figure 7). While striated marks are clearly visible in the top LEA (LEA 1), they are virtually non-existent in the other five LEAs (the only striated marks that can sometimes be seen are the transition between land and groove impression). For this reason, in a desire to analyze

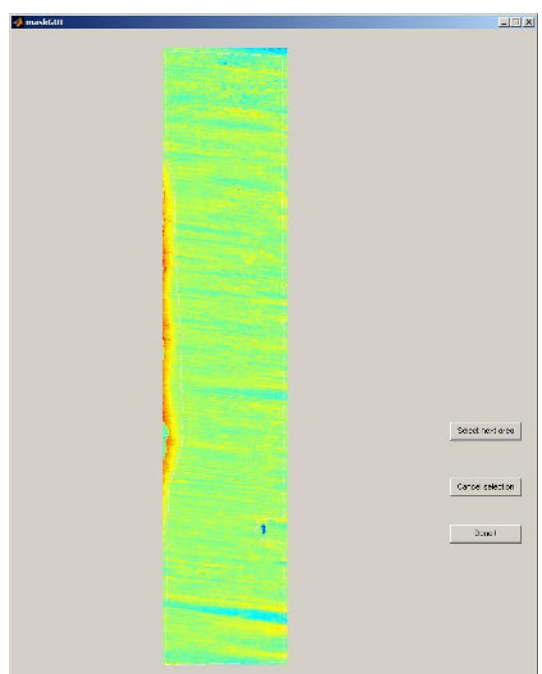

Figure 17: Manual Selection of Region of Interest

bullets fired by poor quality barrels, a "partially automated" version of the pre-processing software was developed. The partially automated version was the same as the fully automated version in all steps but two. In this section we discuss these two steps.

Selection of Region of Interest

After the **Isolation of Region of Interest** step in the fully automated pre-processing sequence, the operator was given the opportunity to further select the region of interest to exclude portions which did not display striations. This selection was performed through a GUI using the mouse (the GUI can be sees in Figure 17). This functionality was incorporated to allow the operator to handle situations where there was a considerable proportion of the LEA surface which did not include striations. The purpose of the operator the flexibility to exclude regions which do not display striations is to minimize the likelihood of contaminating the profile generation process (and therefore, the signature generation).

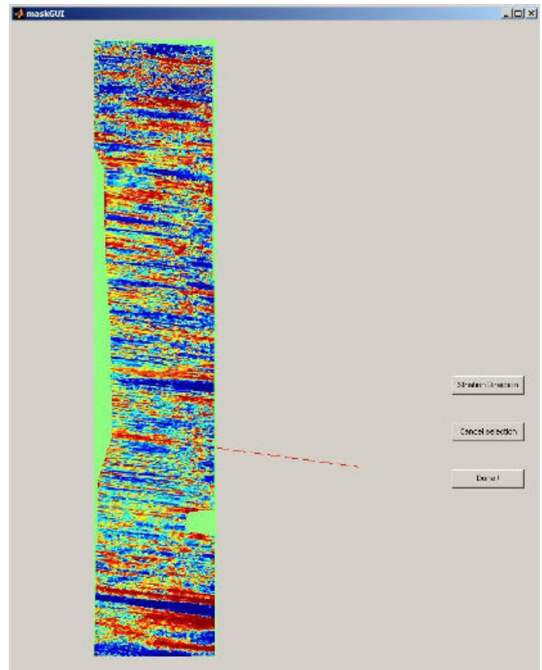

Figure 18: Manual Identification of Rifling Orientation

Identification of Rifling Angle

Once the Manual Selection of Regions of Interest step is completed, the operator is provided with a graphical interface to make a manual identification of the rifling angle. Figure 18 shows the graphical interface used to allow for the manual indication of the rifling angle. To complete this step, the operator manually "draws" a line parallel to the striations (the operator has to only select the beginning point and end point of the line). The system interprets the line drawn by the operator as indicative of the direction along which the striations are oriented. Based on this orientation, the profile generation step is performed.

4.1.2.4 LEA-to-LEA Similarity Measure

As discussed in Section 4.1.2.1, in order to compute the bullet-to-bullet similarity measure it is first necessary to compute the LEA-to-LEA similarity measure for each possible pair of LEAs for the pair of bullets under comparison. The LEA-to-LEA similarity measure is computed according to the following equation:

$$Sim(a,b) = \max_{|\Delta x| < \Delta x_{\max}} \left[1 - \frac{\left\| l_1(x+\Delta x) - l_s(x) \right\|^2}{\left\| l_1(x+\Delta x) + l_s(x) \right\|^2} \right] \quad (1)$$

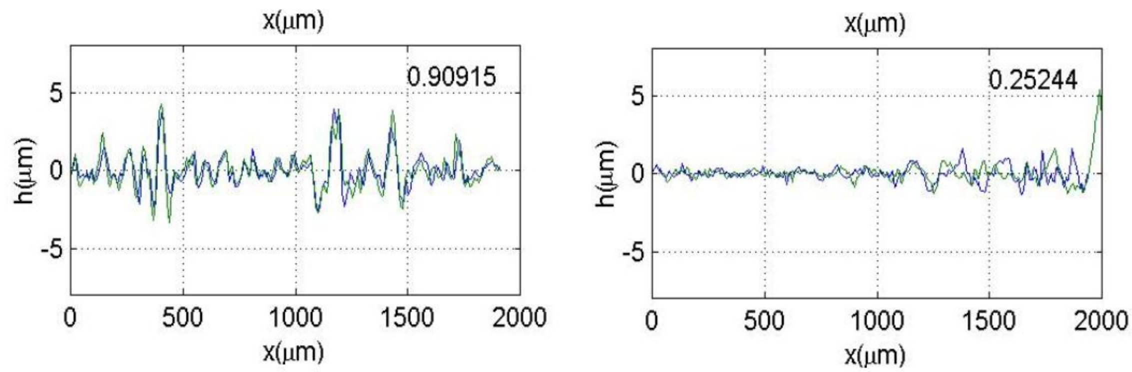

Figure 19: Comparison of signatures corresponding to matching land impressions (left) and non-matching land impressions (right) and the corresponding evaluation of their relative distance similarity metric.

where l_1 and l_2 correspond to the zero-mean one-dimensional signatures associated with the LEAs under comparison, and the norm $\|\bullet\|$ corresponds to the Euclidean norm:

$$\|l\| = \sqrt{\sum l_i^{\,2}} \tag{2}$$

and $\Delta x_{\max}$ is a maximum amount of lateral displacement allowed for comparison. The maximum correlation is found by displacing (shifting) one data set with respect to the other by Δx. This shift is necessary because there is no guarantee that the initial point where data was taken for one LEA is the same as that of the other. We refer to this similarity metric as a "relative distance metric." The relative distance metric is a time-domain similarity metric (as opposed to frequency-domain, wavelet-domain, etc.), and it offers advantages in terms of being suited to deal with signatures of different lengths, as well as signatures with missing data points (dropped points, outliers, etc). An example of the results of the use of this similarity metric in the case of LEAs can be seen in Figure 19, where the similarity value is shown on the upper right corner for comparisons of a pair of matching and non-matching LEAs. Notice the difference in the similarity metric between the matching (left pair; similarity metric: 0.91) and non-matching (right pair; similarity metric: 0.25) LEAs.

4.1.3 Data Selection

The preliminary tasks associated with this project included the selection of the barrel models and ammunition brands that would be used as part of this study. As part of the 2005 NIJ Study, IAI procured barrels of nine different manufacturers spanning the spectrum of manufacturing quality. In most cases, 11 barrels of each make were acquired, and every attempt was made to obtain consecutively manufactured barrels (as seen in Table 2, we were successful in a number of cases). For each of these barrels, a minimum of 24 bullets were test fired (10 pristine and 2 damaged bullets of both Winchester and Remington ammunition), retrieved, and stored for future research.

	Manufacturer	Manufacturing Technique	No. of Barrels	No. of LEAs per bullet	LEA Width [mm]	Notes
1	Browning	Hammer Forged	10	6	1.8	Sequential
2	Bryco	Gang Broach	10	6	1.3	Consecutive
3	HiPoint	Button Rifling	10	9 / 6	1.6 / 1.3	Consecutive
4	SIG	Hammer Forged	10	6	1.7	Consecutive
5	Taurus	Gang Broach	6	6	1.3	Consecutive

Table 2: Detailed information about barrels of interest

The barrel models to be investigated under this study were selected among those barrels used in the 2005 Study on the basis of their quality of manufacture. Barrels representative of both very poor quality and very good quality of manufacture were selected. Among the selected barrels we classify HiPoint, Taurus and Bryco as being representative of barrels of very poor quality of manufacture; and SIG Sauer and Browning as being representative of barrels of very good quality of manufacture. In terms of ammunition, the Winchester ammunition has been selected for the purposes of this study.

Table 2 shows the list of selected barrel models, along with their manufacturing technique, number of barrels selected, number of rifling impressions, and approximate width of the land impressions.

4.1.4 Statistical Analysis

We refer to the distribution of the similarity measure obtained from the comparison of bullets fired by the same barrel as the matching distribution, while we refer to the distribution of bullets fired by different barrels as the non-matching distribution.

Once the matching and non-matching distributions are plotted, it is possible to estimate the probability of identification error associated with the comparison of two bullets. As expected, a clear separation between the matching distribution and the non-matching distribution indicates a low probability of error, while significant overlap between matching distribution and the non-matching distribution indicates a high probability of error associated with the comparison of two bullets. For the purposes of this study, we use the Empirical Probability of Error to quantify the degree to which the matching and non-matching distributions overlap.

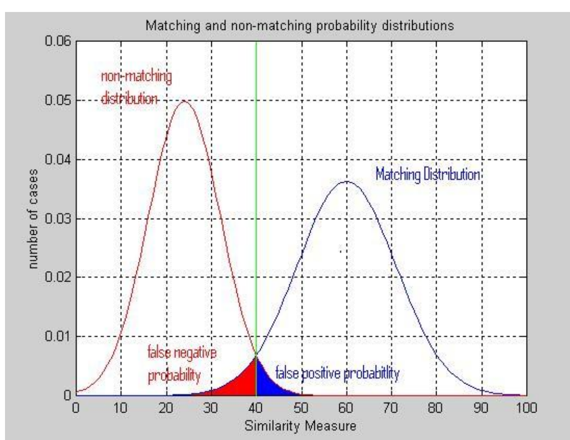

Figure 20: Empirical Estimation of Probability of Orientation Error

Empirical Probability of Error: This approach is probably one of the most classic statistical methods used in conventional Hypothesis Testing problems. Having the empirically generated matching and non-matching bullet-to-bullet similarity distributions for a barrel brand under consideration, it is possible to compute an optimal boundary or threshold such that if a given bullet-to-bullet comparison yields a similarity measure above the threshold, it is assumed to be a matching pair, while any orientation yielding a similarity measure below the threshold is classified as a being a non-matching pair. The boundary or threshold value is selected to minimize the average probability of error (both false positive and false negative). Figure 20 shows a graphical representation of this approach, where two distributions are shown, a matching distribution, and a non-matching distribution. Having identified the optimal threshold, it is possible to estimate the probability of false positive identification, as well as false negative identification. We use the probability of error as a metric of distance between distributions, where the distance is inversely proportional to the empirically computed probability of error.

4.2 Results

In this section we discuss the performance of the automated topography based ballistic analysis system discussed in Section 4.1.1. As we interpret these results, it is import to emphasize that the main objective of this study was not to develop a "perfect" comparison system (although that would have been quite nice too!), but to answer the questions left open by our previous study: **Given that the basic premise of ballistic identification was well validated in an objective, quantifiable manner for barrels of average manufacturing quality, is it possible to extend said validation to bullets fired by barrels of very poor and very good manufacture quality?.** Perhaps another way to pose this question is the following: **Is the fact that reliable identification was not achieved for barrels of very poor and very good manufacture quality due to the deficiencies of the system (and algorithms), or due to the fact that such bullets cannot be identified?** From this perspective, our main goal was to determine whether it was possible to **improve** upon the results of our previous study. If improvement is possible, it would indicate that the deficiencies in our previous study were due to the system used in the study, and not due to the fact that the bullets fired by barrels of "very good" or "poor" manufacture quality cannot be identified. If no improvement is possible, there is the possibility that bullets fired by certain barrel brands (or individual barrels) simply cannot be identified, no matter what means are applied to the task.

Detailed results of our analysis can be found in Appendix B. These results are displayed in two formats: a) by barrel brand, and b) barrel-by-barrel for a given brand. Let us consider as an example the results obtained for Browning barrels. Figure 24 shows the distribution of matching and non-matching pairs of bullets for all bullets fired by all ten Browning barrels (see top of figure). In the body of this plot one can see some of the basic statistical data associated with this distribution, including the estimated empirical probability of error (Pe). The same data is segregated barrel-by-barrel in Figure 26, where the first column of data corresponds to the non-matching distribution, and the remaining columns correspond to the matching distributions of each of the ten barrels used in this analysis. The top of this figure shows the same data, in graphical form.

4.2.1 Barrels of Very Good Manufacturing Quality

For the purposes of this study, Browning and SIG barrels were classified as barrels of very good manufacture quality. The bullets fired by these barrels proved difficult to identify in the 2005 NIJ Study primarily because the striations found on their LEAs were very fine, and proved too small to be acquired by the instrumentation used as part of that study.

Browning:

The ability to identify matching and non-matching pairs of bullets was significantly improved in this study with respect to the 2005 NIJ Study. In the case of fully-automated pre-processing, the Pe decreased from 18.1% to 6.4%. Moreover, in the case of semi-automated pre-processing the Pe decreased even further to 3.0%. The improvement in performance in the case of the fully-automated pre-processing algorithms indicates that the system's ability to isolate the individual features of the LEAs on bullets fired by Browning barrels has been enhanced. The fact that the semi-automated pre-processing did not yield significant improvements over the fully-automated pre-processing indicates that the identification of regions of good quality (where striations are clear) on the surface of the LEAs had relatively little impact for this barrel brand. This is an area where additional improvement can be made.

SIG:

As in the case of Browning barrels, the ability to identify matching and non-matching pairs of bullets fired by SIG barrels was significantly improved with respect to the 2005 NIJ Study. In the case of fully automated pre-processing, the Pe decreased from 45.2% (which, out of a worse case of 50% is almost as good as guessing) to 31.4%. In addition, in the case of semi-automated pre-processing the Pe decreased even further to 25.7%. The fact that the semi-automated pre-processing has a significant impact seems to indicate that the identification of regions of good quality on the LEAs surface had a significant impact in the case of these barrels. This points to the fact that further performance improvements are possible by developing suitable algorithms to identify said good regions (IAI invested considerable effort in the development of such algorithms, which proved too challenging for the available time and resources).

4.2.2 Barrels of Poor Manufacturing Quality

For the purposes of this study, Taurus, HiPoint and Bryco barrels were classified as barrels of poor manufacture quality. The bullets fired by these barrels proved extremely difficult to identify in the 2005 NIJ Study. The difficulties associated with these barrel brands were related to the fact that the LEAs found on the bullets fired by them were often not well defined, making it difficult to identify the boundaries between a LEA and a GEA. More importantly, the striations found on these LEAs were often not clearly defined.

Taurus:

The ability to identify matching and non-matching pairs of bullets was significantly improved in this study with respect to the 2005 NIJ Study. In fact, one could argue that the classification of Taurus as a barrel of poor manufacture quality was perhaps wrong, and it should be considered a "middle of the road" barrel. In the case of fully-automated pre-processing, the Pe decreased from 17.6% to 6.8% with respect to the previous 2005 NIJ Study. The case of semi-automated pre-processing did not improve the Pe significantly, but only down to 7.6%. In other words, basically the same performance as that obtained with fully-automated pre-processing. The improvement in performance in the case of the fully-automated pre-processing algorithms indicates that the system's ability to isolate the individual features of the LEAs on bullets fired by Taurus barrels has been enhanced. The fact that the semi-automated pre-processing did not yield significant improvement over the fully-automated pre-processing indicates that the identification of regions of good quality (where striations are clear) on the surface of the LEAs had relatively little impact for this barrel brand.

HiPoint:

The improvement in our ability to identify matching and non-matching pairs of bullets fired by HiPoint barrels was not improved as part of this study. In the case of fully-automated pre-processing, the achieved Pe was 36.9% as opposed to 36.3% in the 2005 NIJ Study. Our attempts to do a semi-automated pre-processing of these bullets did not yield a better result. After much effort, we decided to consult with firearms examiner Martin Ols of ATF regarding this bullets. With the assistance of Firearms Examiner Ols and after looking at some of these bullets under the comparison microscope it became clear to us that the key reason that we had not been successful with the comparison of these bullets probably lied on the fact that the LEAs of these bullets have most of useful striations close to the transition between LEA and GEA. While our success with this barrel brand was very limited, it is the opinion of the author that bullets fired by these barrels can be identified reliably.

Bryco:

The improvement in our ability to identify matching and non-matching pairs of bullets fired by Bryco barrels was not improved as part of this study. In the case of fully-automated pre-processing, the achieved Pe was 46.5% as opposed to 47.1% in the 2005 NIJ Study. These numbers pretty much indicate that a reliable identification of these bullets would not have been possible with the set of algorithms used in either study. Neither the improved imaging resolution nor any other efforts we undertook had any effect. Perhaps this outcome can best be explained by simply looking at the LEAs found on these bullets. A good example is shown in Figure 7, where a photorealistic rendering of the LEAS found on one such bullet are shown. As seen in this image, the LEAs are highly inconsistent; even in their width. There is considerable evidence of "skidding", a phenomena where the bullet does not make good contact with the interior of the barrel, resulting in the bullet skidding inside the barrel. Moreover, only one LEA shown in Figure 7 shows much evidence of striations. An inspection of the Bryco barrels through which these bullets were fired reveals that even these barrels are highly irregular. The lands on these barrels have varying depth as one looks along the axis of the barrel. It is therefore not surprising that the bullets fired by these barrels are highly irregular. This is further confirmed by our results in the measurement of the GEA-to-GEA diameter (see Section 4.3). As will be discussed in that section the variation in GEA-to-GEA diameter of these bullets was considerably greater than for any other barrel brand.

Remarks:

Even in the case of Bryco barrels, it is not accurate to make sweeping statements such as: "bullets fired by barrels of X brand can or cannot be identified". The fact of the matter is that the ability to determine that a given bullet was fired by a specific barrel very much depends on the barrel itself; and not only in the brand of its manufacture. Figure 37 shows a particularly good example of this case. As seen in this analysis of the barrel-by-barrel performance in the analysis of SIG barrels, there can be considerable differences between barrels of the same brand. In the case of Figure 37, one can observe that the bullets fired by the first two barrels were correctly classified (labeled barrel B 2 and B 3), while bullets fired by the rest of the barrels would have most likely been difficult to classify. This is not necessarily surprising. A typical scenario is a barrel which has some unique feature resulting from either manufacture or use (perhaps a deep scratch generated during manufacture or a defect in the crown, possibly from careless handling of it). In other words, while we can say that certain barrel brands will in general transfer less consistent features to the bullets fired by them, one should never generalize such statement to mean that no barrel of a given manufacture can ever be matched.

The results of the present study show quantifiable improvements with respect to the previous 2005 NIJ Study. Most importantly, the improvement in classification performance for SIG, Browning and Taurus provides strong evidence that bullets fired by these brands of barrels can be classified with a satisfactorily low probability of error. This is especially true when one considers that a trained human Firearms Examiner will without a doubt perform better than an automated system (at least in the conceivable future). This statement is most likely to remain true for two main reasons: Humans have a remarkable ability to perform "pattern matching", and such ability will be difficult to replicate by any automated system. Furthermore, an automated system relies on taking into consideration only certain portions of the bullet under analysis (for the foreseeable future), while a human Firearms Examiner can always look for corroborating evidence in different portions of the bullet.

While much progress and improvement was achieved during this study, there is much that was not possible to complete within its time and resources constraints. It is the impression of the author that while great progress was made in the pre-processing algorithms; there is still room for improvement; especially in the identification of poor quality LEA portions (portions of the LEA that do not contain striations), and in the identification and classification of striations. In addition, there is also considerable room for improvement in the development of new correlation algorithms.

4.3 Relationship between barrel characteristics and performance

An additional goal of this project is to attempt to improve our understanding of the parameters associated with the individuality of the features transferred between a barrel and bullets fired through it. Among these parameters, it is reasonable to expect that the diameter of a fired bullet would provide an indication of the pressure acting on the bullet as it traverses the barrel. The GEA-to-GEA diameter (diameter measured from one groove to the one on the opposite side) also has the advantage of being relatively easy to measure.

Fired by		Groove-to-groove diameter	
Gun Brand	Code	Mean (x 0.1 inch)	Standard Deviation (x 0.1 inch)
Taurus	A	3.534	0.005
Hipoint	B	3.512	0.008
Bryco	D	3.506	0.011
Ruger	E	3.512	0.004
S&W	H	3.498	0.005
Beretta	I	3.511	0.005
Sig	F	3.517	0.003
Browing	G	3.520	0.007
Pristine	P	3.599	0.003

Table 3: Mean and Standard Deviation (in tenths of inches) of bullet GEA-to-GEA diameter by brand

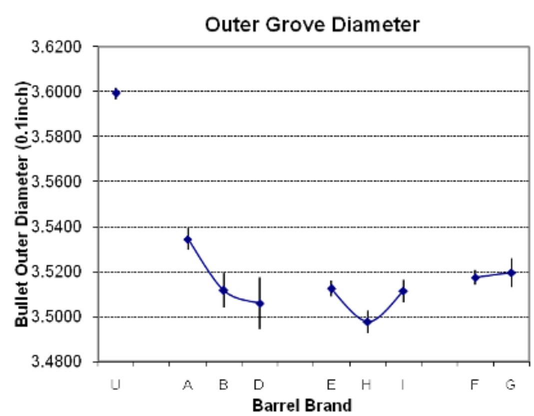

Figure 21: Distribution of GEA-to-GEA diameters by brands

In order to investigate this issue, the dimensions of fired bullets from eight barrel brands, as well as that of pristine bullets, have been carefully measured. The bullets in this study are manufactured by Winchester. The eight gun brands for which measurements were taken were Taurus(A), Hipoint(B), Bryco(D), Ruger(E), S&W(H), Beretta(I), Sig(F), and Browning(G). Five barrels were chosen for each brand. The GEA-to-GEA diameter of three bullets fired by each barrel was measured. For each bullet three grove-to-groove measurements were made. Each measurement was conducted twice.

Table 3 summarizes the results of these measurements (also shown in graphical manner in Figure 21). Notice that we included Ruger, S&W and Beretta, brands for which we know that the transfer of unique features between barrel and bullet is very good. Figure 21 shows this information in four groups: the first group from the left is a singleton, and it corresponds to an unfired bullet (labeled P). The second group corresponds to those barrels which have been considered to be of poor manufacture quality; Taurus, HiPoint and Bryco (labeled A, B and D respectively). The third group corresponds to those barrels which are considered to be "middle of the road"; Ruger, S&W and Beretta (labeled E, H and I respectively). Finally, the fourth group corresponds to those barrels considered to be of high manufacture quality; SIG and Browning (F and G respectively). It is worth reminding the reader at this point that this classification is not meant to be an assessment of the barrel or gun functional quality, but simply an assessment of the manner in which features are transferred between the barrel and the bullets fired by it.

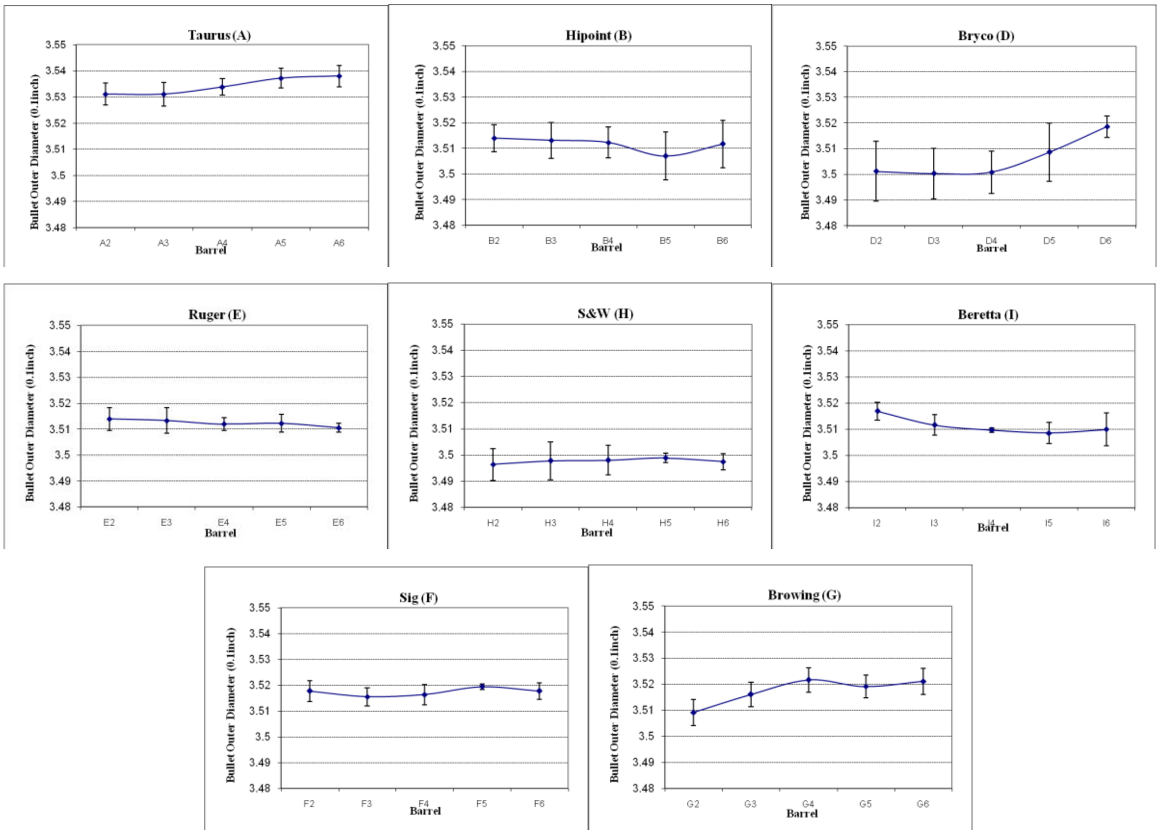

Figure 22: distribution of GEA-to-GEA diameter by brand and barrel.

The first remark to be made based on the data shown in Table 3 is that for all barrels under comparison, the GEA-to-GEA diameter of fired bullets is less than that of an unfired bullet. This is not a surprising observation, as the bullet must be pressed upon by the barrel in order to maintain contact with it.

A more interesting observation is that there appears to be a correlation between the barrel manufacturing quality and the standard deviation of the diameters of the bullets. As seen in Table 3, the highest standard deviations were recorded for barrels of Bryco (1.1 mils) and HiPoint (.8 mils) manufacture. As was discussed in the previous section, these two barrel brands proved to be the most challenging due to the poor transference of features between the barrel and the bullets fired by them. Notice, however that the standard deviation reported in Table 3 originates from two different sources of variation: a) the variation of geometrical dimensions among the barrels through which the bullets were fired, and b) the variation of the dimensions of the bullets fired by each individual barrel. The question is then: are the different barrels of a given brand all equal, or are there significant variations for barrels of the same brand?

Figure 22 shows the mean and standard deviation of GEA-to-GEA diameters for each of the 5 barrels evaluated, for each of the brands under consideration. Notice that as expected, there is variation between barrels (the mean value of the GEA-to-GEA diameter is different for different barrels) and within barrels (the standard deviation of the diameter is significant even among bullets fired by the same barrel). Notice that the range of variability in the mean diameter value between barrels is similar for all barrel brands (with the exception of Bryco, which shows greater range of variability). However, the variability of diameters among bullets fired by the same barrel is in general greater for Bryco and HiPoint, the barrels of lowest quality of manufacture.

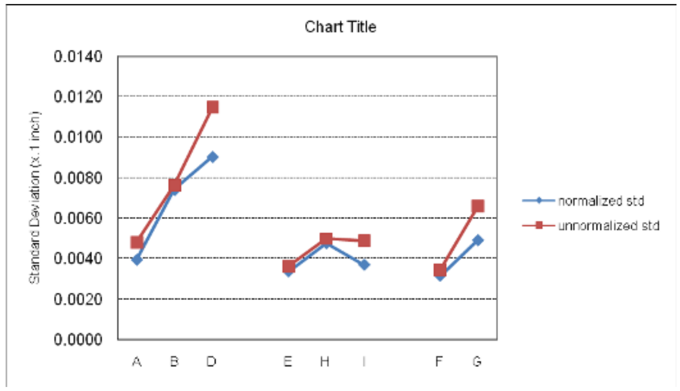

Figure 23: normalized and un-normalized standard deviation of GEA-to-GEA bullet diameters

Figure 23 shows a plot of the GEA-to-GEA diameter standard deviation due to both barrel diameter variability and bullet variability (un-normalized standard deviation) and also the standard deviation due to bullet variability only (normalized). As seen in Figure 23, the contribution of barrel variability is minor when compared to the variability among bullets themselves. As discussed above, the two barrels which display the greatest variability (both normalized and un-normalized) are Bryco and HiPoint. Notice that this variability becomes more pronounced once we normalize for the barrel-to-barrel variability. This is evidence of significant groove-to-groove diameter inconsistencies even among bullets fired by the same barrel.

As was discussed in the Results Section, the comparison of bullets fired by Bryco barrels proved to be the most challenging of all; followed by the comparison of bullets fired by HiPoint barrels. The results of our comparison of GEA-to-GEA diameters provides evidence to the fact that bullets fired by Bryco barrels (and to a lesser extent by a HiPoint barrel) display significant inconsistencies, even when fired by the same barrel.

4.4 Modifications of project or problems

No significant modifications took place during this project. In terms of problems, the identification of poor quality striated regions on the bullet's LEAs proved more difficult than expected, and we did not succeed to develop algorithms which functioned to our satisfaction given the time and resources limitations of the project. This is by no means a criticism of these limitations, but an acknowledgement of the level of difficulty of these challenges. For this reason, a semi-automated pre-processing option was developed. This pre-processing path allowed us to manually select the LEA regions which showed most promise. The semi-automated approach is not optimal (because it requires human intervention, taking away some of the objectivity of the study), but for the most it served the desired purpose; which was to show that the identification of LEA regions of good quality can improve the result of classification analysis.

5. Conclusions

The main question to be addressed by this study was the following:

> *Given that the basic premise of ballistic identification was well validated in an objective, quantifiable manner for barrels of average manufacturing quality, is it possible to extend said validation to bullets fired by barrels of very poor and very good manufacture quality?*

At the completion of this study, we can confidently say that the above statement can be extended to barrels of very good manufacture quality such as SIG, and Browning. Further, it can also be extended to Taurus. The evidence is provided by the fact that significant improvement was achieved in terms of correctly identifying bullets fired by these barrels with respect to the results obtained in the previous 2005 NIJ Study. This improvement was possible thanks to the use of an instrument of superior performance to the one used in the 2005 Study, and to the development of better pre-processing algorithms. This suggests that the limitations of the 2005 NIJ Study were not associated with the barrels/bullets themselves, but with the system used to do the analysis. While we were not successful in extending this conclusion to HiPoint and Bryco barrels, it is the impression of the author that given additional time and resources it can be shown that bullets fired by HiPoint barrels can also be successfully identified. This is not necessarily the case for Bryco barrels. Even though in the case of gun barrels of poor quality the use of a better instrument did provide the ability to identify good and bad portions of the LEAs, it was noticed that in many cases LEAs of bullets fired by such guns barely displayed any striations, or (as in the case of Bryco) only one LEA out of 6 had any meaningful striations. This seems to indicate that the pressure exerted by the barrel on the bullet was not even around the entire bullet, suggesting the possibility (long speculated) that the flight path of the bullets within the barrel is not the same for every firing. In addition, in the case of Bryco, we have found significant evidence of considerable variability (as discussed in Section 4.3), and it is likely that bullets fired by barrels of such poor manufacture quality will never be amenable to reliable identification.

Another important conclusion is that it is not accurate to make sweeping statements such as: "bullets fired by barrels of X brand can or cannot be identified". The fact of the matter is that the ability to determine that a given bullet was fired by a specific barrel very much depends on the barrel itself; and not only in the brand of its manufacture. This is not necessarily surprising. A typical scenario is a barrel which has some unique feature resulting from either manufacture or use (perhaps a deep scratch generated during manufacture or a defect in the crown, possibly from careless handling of it). In other words, while we can say that certain barrel brands will in general transfer less consistent features to the bullets fired by them, one should never generalize such statement to mean that no barrel of a given manufacture can ever be matched.

It is important to keep in mind that a trained human Firearms Examiner will without a doubt perform better than any automated system (at least in the conceivable future). This statement is most likely to remain true for two main reasons: Humans have a remarkable ability to perform "pattern matching", and such ability will be difficult to replicate by any automated system. Furthermore, an automated system relies on taking into consideration only certain portions of the bullet under analysis (for the foreseeable future); while a human Firearms Examiner can always look for corroborating evidence in different portions of the bullet.

Finally, this study has given us the opportunity to "look" at what can be considered challenging LEAs, and we have learned much from this experience. It has become clear to us that the next step in automated ballistic identification techniques will require a different approach to the characterization of the LEAs (or the signature generation process). Similarly, innovations will be required in the correlation of these signatures. We look forward to the opportunity to undertake such challenge.

6. Appendix A: References

[1] DAUBERT v. MERREL DOW PHARMACEUTICALS, 509 U.S. 579 (1993).

[2] KUMHO TIRE CO. v. CARMICHAEL, 526 U.S. 137 (1999).

[3] "Development of a 3D-based Automated Firearms Evidence Comparison System," B. Bachrach, Journal of Forensic Sciences, November 2002, Vol 47, No 6, pp. 1253.

[4] "A Statistical Validation of the Individuality of Guns Using 3D Images of Bullets," NIJ Contract No. 97-LB-VX-008, Final Report.

[5] L. Hong, Y. Wang, and A. K. Jain, "Fingerprint image enhancement: algorithm and performance evaluation," Transaction on PAMI, 21(4), 1998, pp. 777-789

7. Appendix B

7.1 BROWNING

The following distributions correspond to Browning barrels. Figure 24 corresponds to the fully automated pre-processing. Figure 25 corresponds to the semi-automated pre-processing. Figure 26 and Figure 27 correspond to the barrel-by-barrel results.

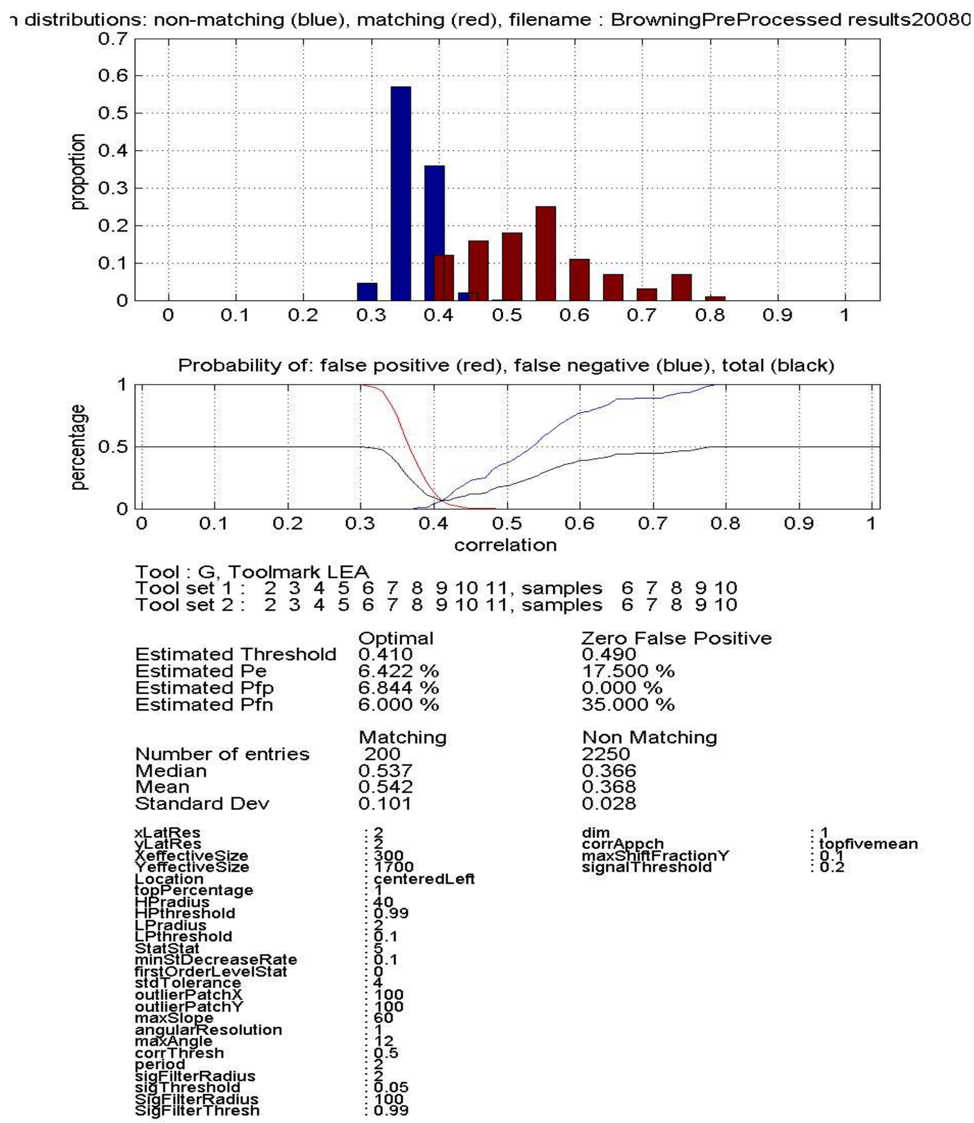

Figure 24: Filename G_LEA_distribution_20080314T013152.jpg, automated processing

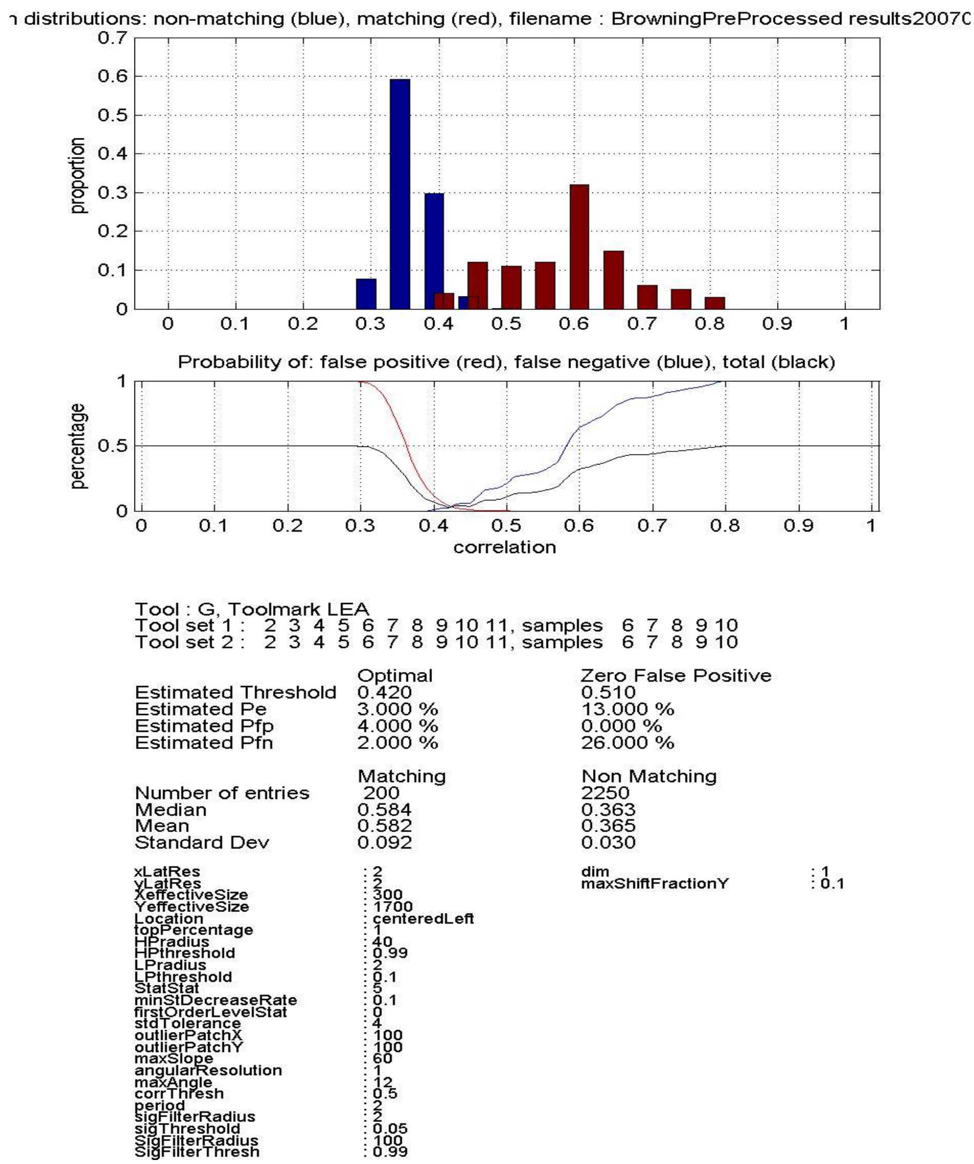

Figure 25: Filename: G_LEA_distribution_20080314T143731.jpg using manual region selection

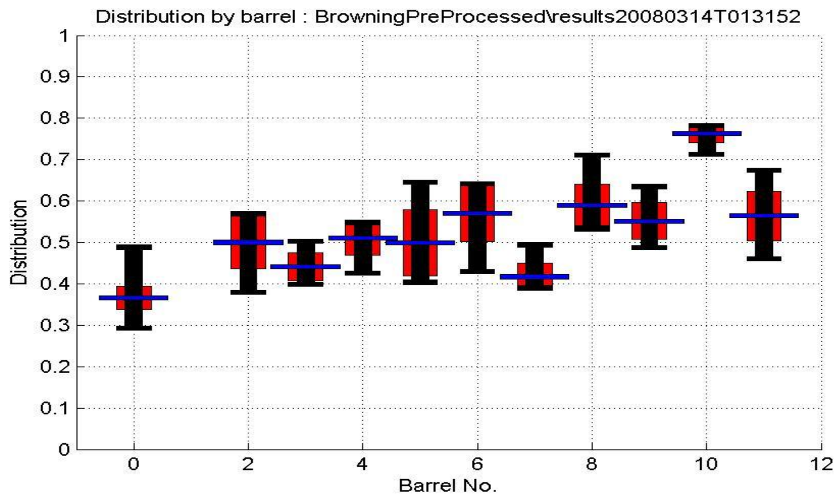

Tool : G, Toolmark LEA
Tool set 1 : 2 3 4 5 6 7 8 9 10 11, samples 6 7 8 9 10
Tool set 2 : 2 3 4 5 6 7 8 9 10 11, samples 6 7 8 9 10

	Non match	B 2	B 3	B 4	B 5	B 6	B 7	B 8	B 9	B 10	B 11
Mean	0.368	0.499	0.446	0.496	0.515	0.552	0.429	0.598	0.566	0.755	0.564
Median	0.366	0.500	0.441	0.511	0.499	0.571	0.417	0.590	0.552	0.763	0.564
Stdev	0.028	0.063	0.034	0.042	0.080	0.068	0.032	0.051	0.044	0.022	0.060
Min	0.293	0.379	0.399	0.427	0.404	0.430	0.390	0.533	0.487	0.713	0.461
Max	0.489	0.571	0.503	0.547	0.645	0.642	0.494	0.711	0.635	0.782	0.675
N	2250	20	20	20	20	20	20	20	20	20	20

xLatRes	: 2	dim	: 1
yLatRes	: 2	corrAppch	: topfivemean
XeffectiveSize	: 300	maxShiftFractionY	: 0.1
YeffectiveSize	: 1700	signalThreshold	: 0.2
Location	: centeredLeft		
topPercentage	: 1		
HPradius	: 40		
HPthreshold	: 0.99		
LPradius	: 2		
LPthreshold	: 0.1		
StatStat	: 5		
minStDecreaseRate	: 0.1		
firstOrderLevelStat	: 0		
stdTolerance	: 4		
outlierPatchX	: 100		
outlierPatchY	: 100		
maxSlope	: 60		
angularResolution	: 1		
maxAngle	: 12		
corrThresh	: 0.5		
period	: 2		
sigFilterRadius	: 2		
sigThreshold	: 0.05		
SigFilterRadius	: 100		
SigFilterThresh	: 0.99		

Figure 26: Filename G_LEA_byBarrel_20080314T013152.jpg using automated processing

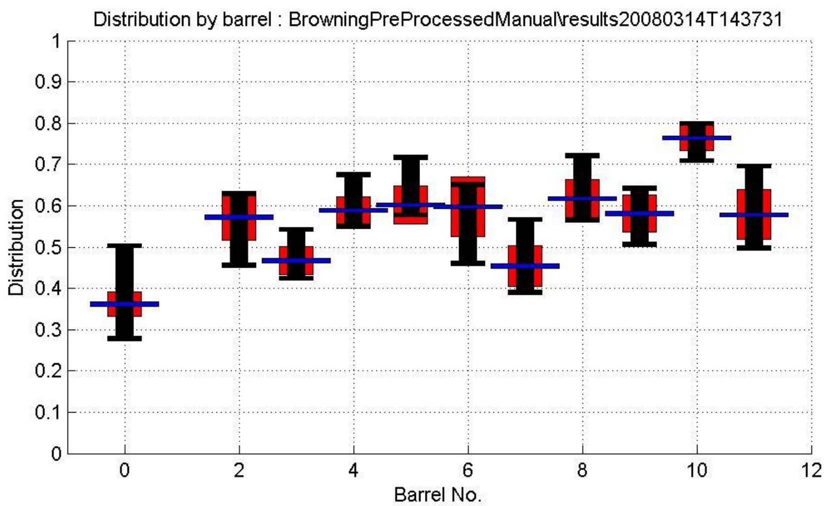

Tool : G, Toolmark LEA
Tool set 1 :   2 3 4 5 6 7 8 9 10 11, samples   6 7 8 9 10
Tool set 2 :   2 3 4 5 6 7 8 9 10 11, samples   6 7 8 9 10

	Non match	B 2	B 3	B 4	B 5	B 6	B 7	B 8	B 9	B 10	B 11
Mean	0.364	0.561	0.476	0.597	0.624	0.571	0.456	0.620	0.583	0.758	0.579
Median	0.362	0.572	0.467	0.589	0.602	0.597	0.454	0.618	0.582	0.764	0.578
Stdev	0.030	0.055	0.035	0.033	0.047	0.072	0.050	0.046	0.045	0.031	0.061
Min	0.278	0.456	0.424	0.551	0.578	0.460	0.391	0.564	0.506	0.710	0.498
Max	0.503	0.629	0.543	0.675	0.717	0.651	0.567	0.721	0.642	0.800	0.697
N	2250	20	20	20	20	20	20	20	20	20	20

xLatRes	: 2	dim	: 1
yLatRes	: 2	corrAppch	: topfivemean
XeffectiveSize	: 300	maxShiftFractionY	: 0.1
YeffectiveSize	: 1700	signalThreshold	: 0.2
Location	: centeredLeft		
topPercentage	: 1		
HPradius	: 40		
HPthreshold	: 0.99		
LPradius	: 2		
LPthreshold	: 0.1		
StatStat	: 5		
minStDecreaseRate	: 0.1		
firstOrderLevelStat	: 0		
stdTolerance	: 4		
outlierPatchX	: 100		
outlierPatchY	: 100		
maxSlope	: 60		
angularResolution	: 1		
maxAngle	: 12		
corrThresh	: 0.5		
period	: 2		
sigFilterRadius	: 2		
sigThreshold	: 0.05		
SigFilterRadius	: 100		
SigFilterThresh	: 0.99		

Figure 27: Filename G_LEA_byBarrel_20080314T143731.jpg using manual region selection

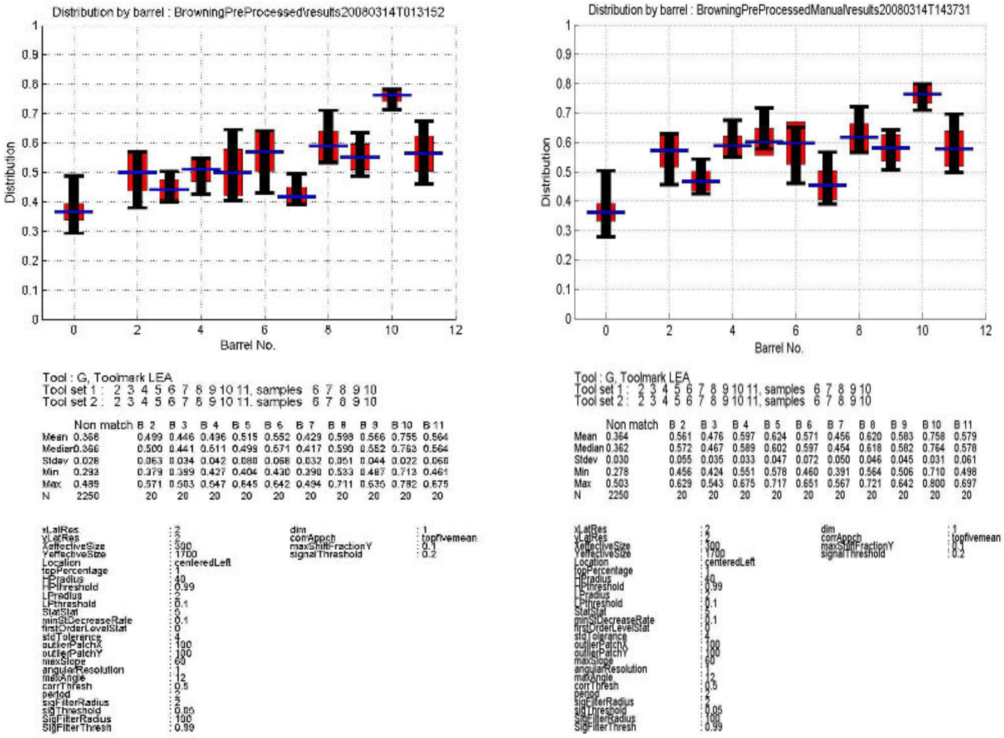

Figure 28: barrel-by-barrel automated vs. semi-manual side by side

7.2 TAURUS

The following distributions correspond to Taurus barrels. Figure 29 corresponds to the fully automated pre-processing; no manual selection of regions of interest or striation orientations. Figure 30 corresponds to the semi-automated pre-processing. Figure 31 and Figure 32 correspond to the barrel-by-barrel results.

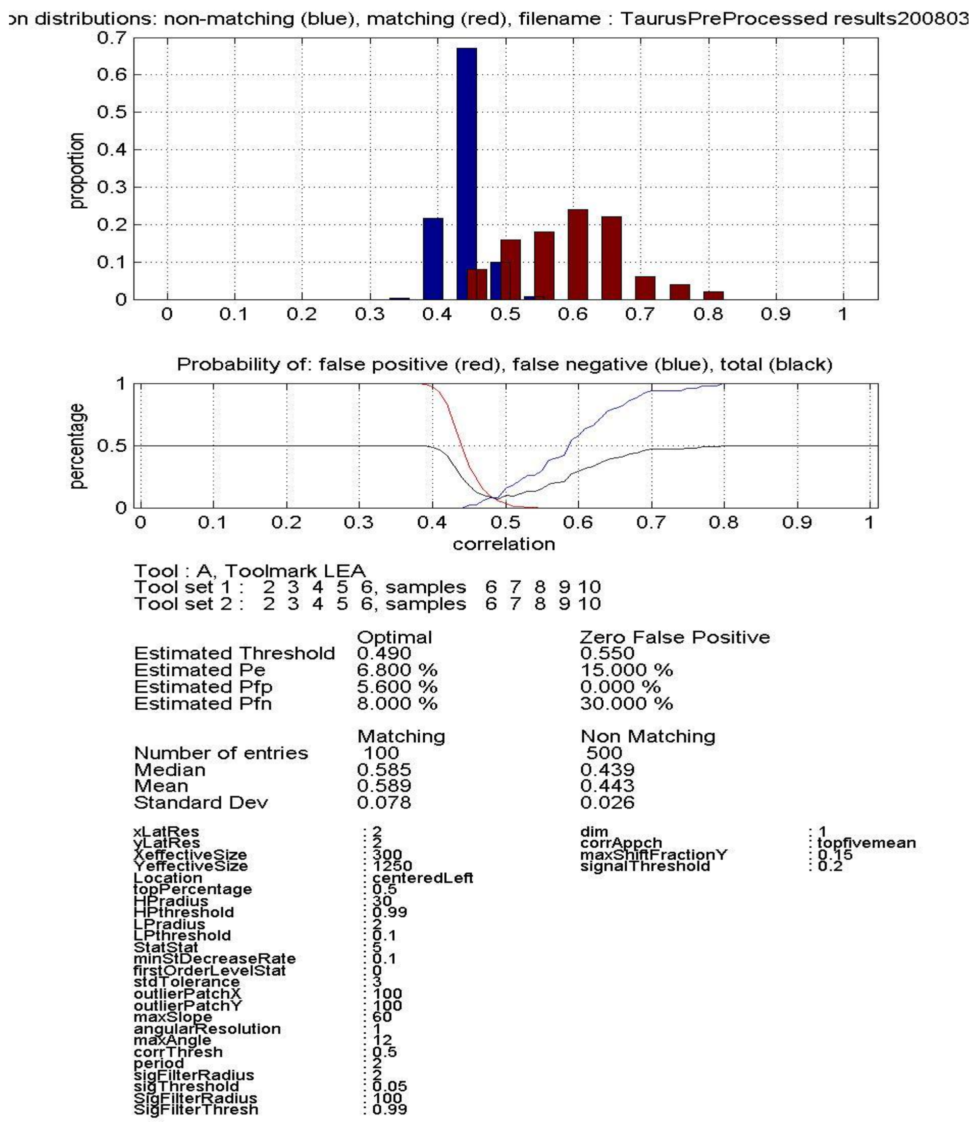

Figure 29: Filename A_LEA_distribution_20080314T004757.jpg, automated processing

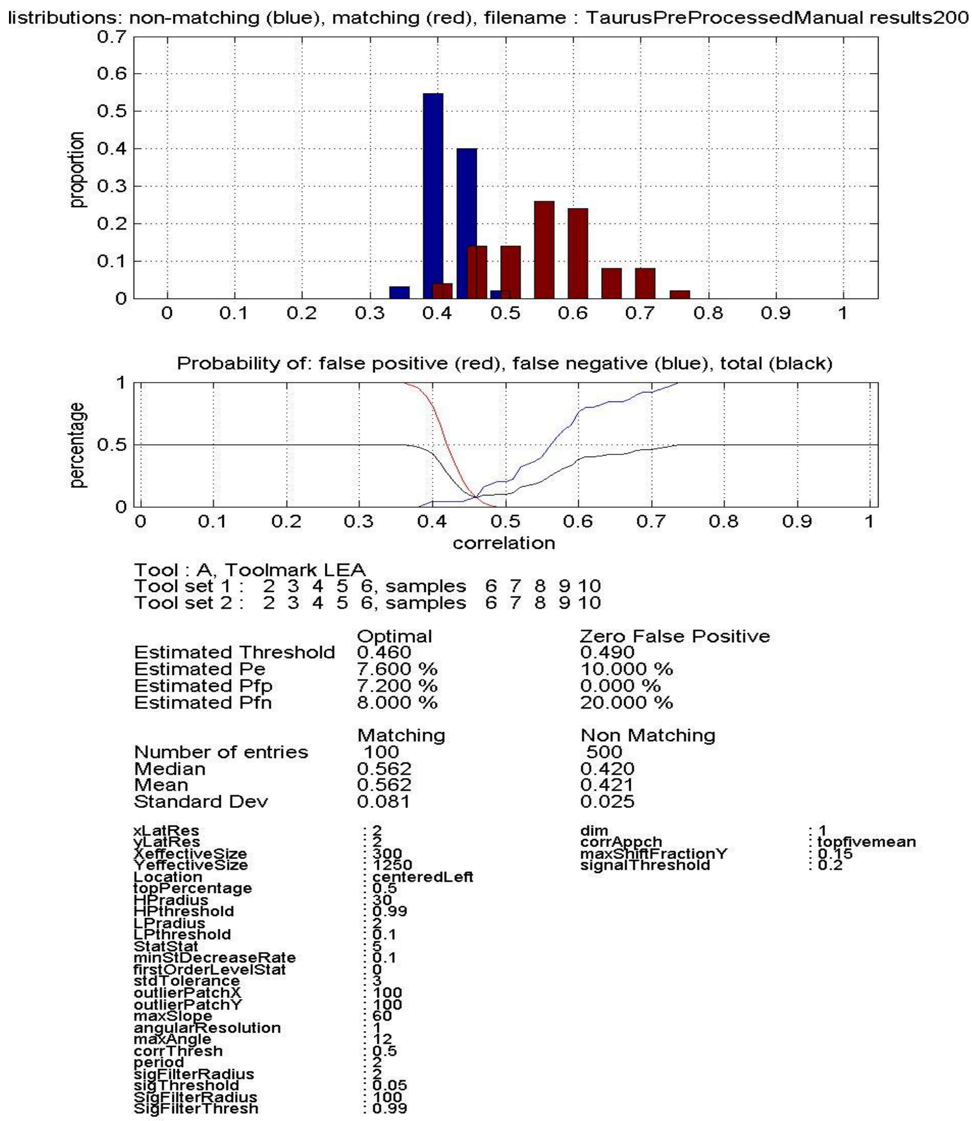

Figure 30: Filename: A_LEA_distribution_20080314T010522.jpg, manually selected by Ben

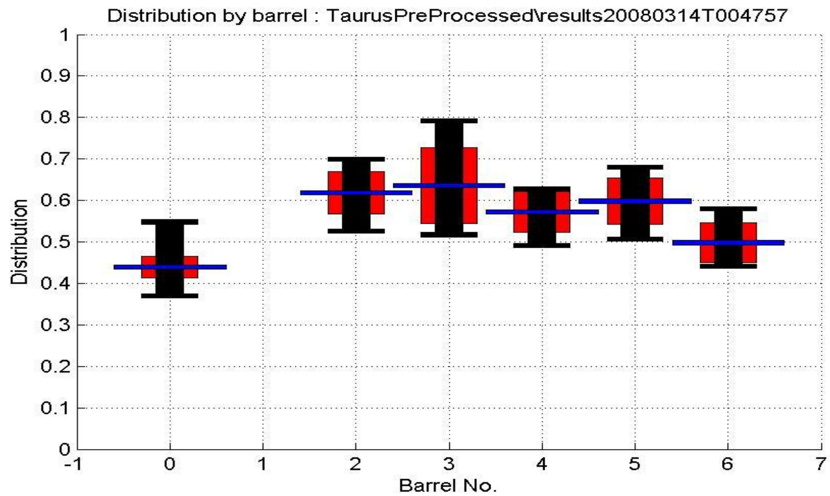

Tool : A, Toolmark LEA
Tool set 1 : 2 3 4 5 6, samples 6 7 8 9 10
Tool set 2 : 2 3 4 5 6, samples 6 7 8 9 10

	Non match	B 2	B 3	B 4	B 5	B 6
Mean	0.443	0.621	0.649	0.566	0.602	0.507
Median	0.439	0.618	0.636	0.573	0.598	0.498
Stdev	0.026	0.052	0.091	0.049	0.056	0.049
Min	0.370	0.527	0.517	0.492	0.507	0.441
Max	0.548	0.699	0.791	0.627	0.681	0.581
N	500	20	20	20	20	20

xLatRes	: 2	dim	: 1
yLatRes	: 2	corrAppch	: topfivemean
XeffectiveSize	: 300	maxShiftFractionY	: 0.15
YeffectiveSize	: 1250	signalThreshold	: 0.2
Location	: centeredLeft		
topPercentage	: 0.5		
HPradius	: 30		
HPthreshold	: 0.99		
LPradius	: 2		
LPthreshold	: 0.1		
StatStat	: 5		
minStDecreaseRate	: 0.1		
firstOrderLevelStat	: 0		
stdTolerance	: 3		
outlierPatchX	: 100		
outlierPatchY	: 100		
maxSlope	: 60		
angularResolution	: 1		
maxAngle	: 12		
corrThresh	: 0.5		
period	: 2		
sigFilterRadius	: 2		
sigThreshold	: 0.05		
SigFilterRadius	: 100		
SigFilterThresh	: 0.99		

Figure 31: Filename A_LEA_byBarrel_20080314T004757.jpg, automated processing

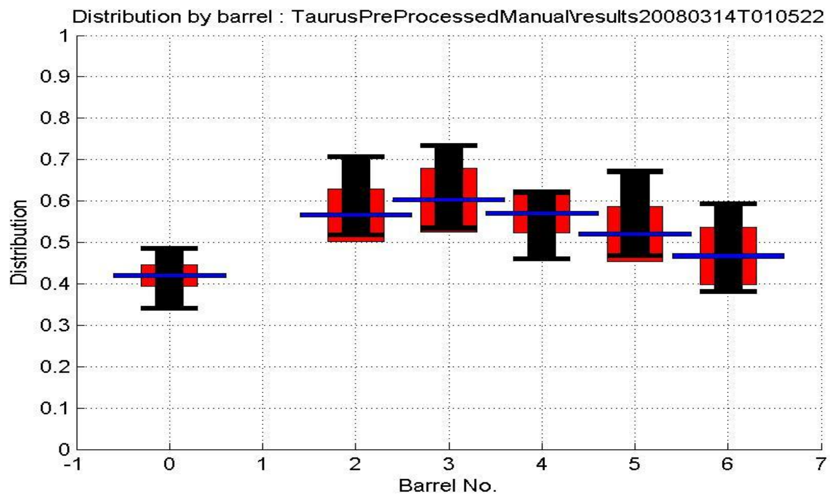

Tool : A, Toolmark LEA
Tool set 1 : 2 3 4 5 6, samples 6 7 8 9 10
Tool set 2 : 2 3 4 5 6, samples 6 7 8 9 10

	Non match	B 2	B 3	B 4	B 5	B 6
Mean	0.421	0.593	0.628	0.559	0.551	0.481
Median	0.420	0.566	0.602	0.571	0.520	0.467
Stdev	0.025	0.063	0.078	0.047	0.066	0.069
Min	0.341	0.519	0.535	0.461	0.469	0.382
Max	0.486	0.707	0.734	0.621	0.672	0.593
N	500	20	20	20	20	20

xLatRes	: 2	dim	: 1
yLatRes	: 2	corrAppch	: topfivemean
XeffectiveSize	: 300	maxShiftFractionY	: 0.15
YeffectiveSize	: 1250	signalThreshold	: 0.2
Location	: centeredLeft		
topPercentage	: 0.5		
HPradius	: 30		
HPthreshold	: 0.99		
LPradius	: 2		
LPthreshold	: 0.1		
StatStat	: 5		
minStDecreaseRate	: 0.1		
firstOrderLevelStat	: 0		
stdTolerance	: 3		
outlierPatchX	: 100		
outlierPatchY	: 100		
maxSlope	: 60		
angularResolution	: 1		
maxAngle	: 12		
corrThresh	: 0.5		
period	: 2		
sigFilterRadius	: 2		
sigThreshold	: 0.05		
SigFilterRadius	: 100		
SigFilterThresh	: 0.99		

Figure 32: Filename: A_LEA_byBarrel_20080314T010522.jpg, manually selected by Ben

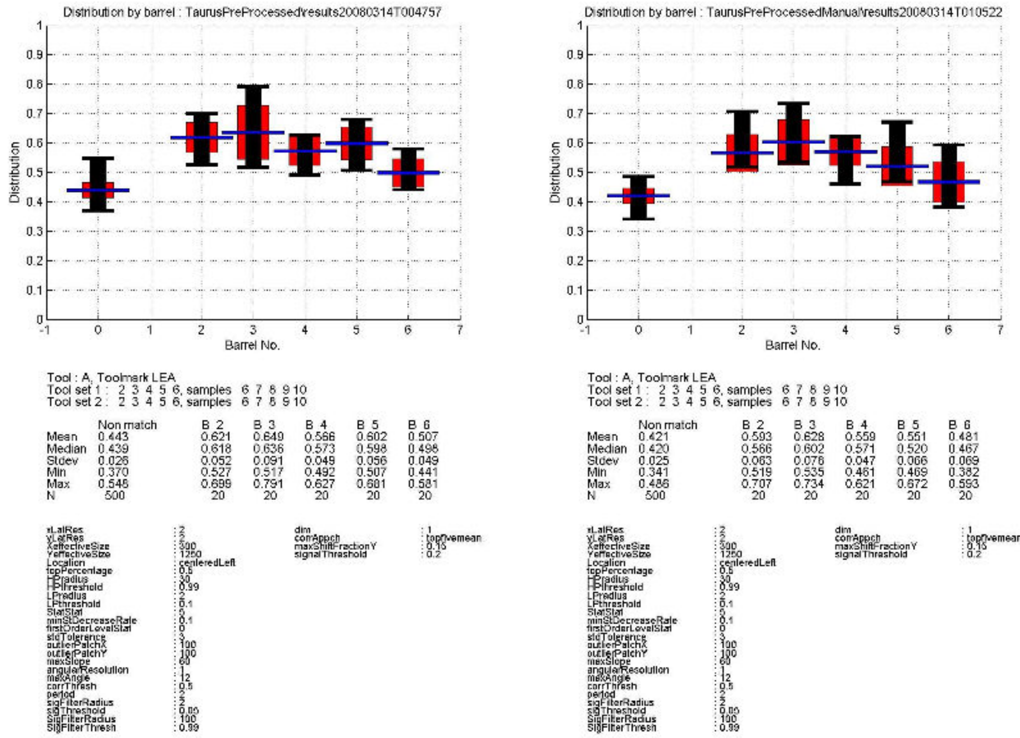

Figure 33: barrel-by-barrel automated vs. semi-manual side by side

7.3 SIG

The following distributions correspond to SIG barrels. Figure 34 corresponds to the automated processing; no manual selection of regions of interest or striation orientations. Figure 35 were processed after manual selection of region of interest. Figure 36

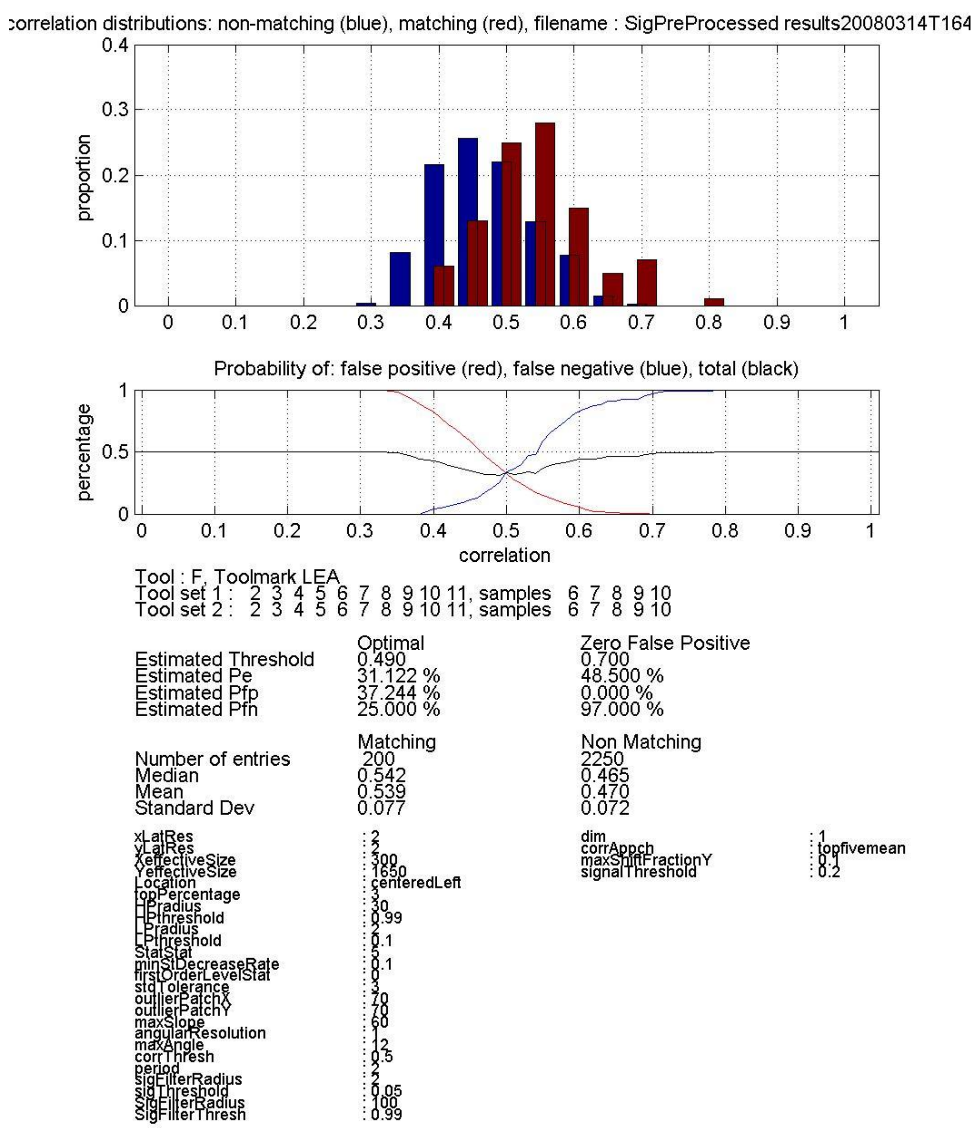

Figure 34: Filename F_LEA_distribution_20080314T164306.jpg, automated processing

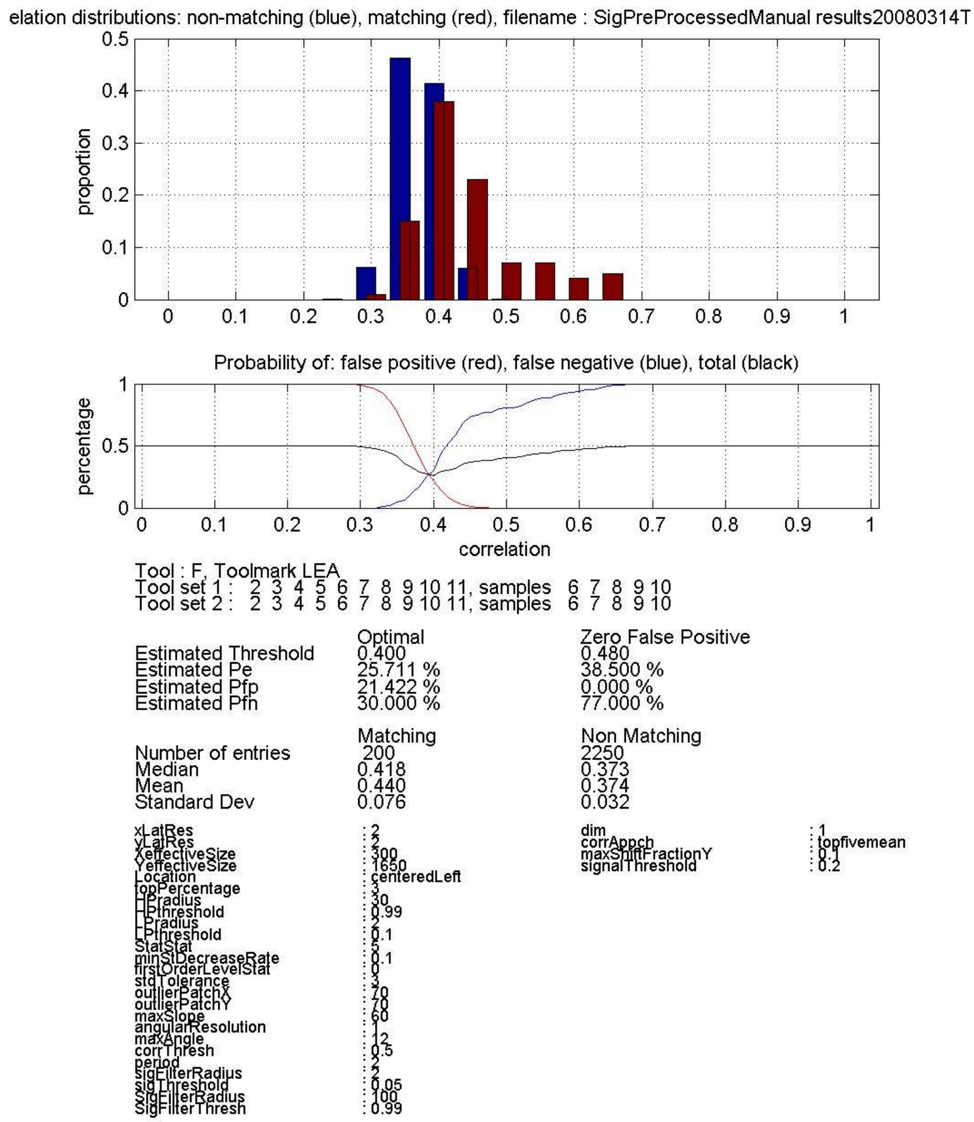

Figure 35: Filename F_LEA_distribution_20080314T154402, using manual region selection.

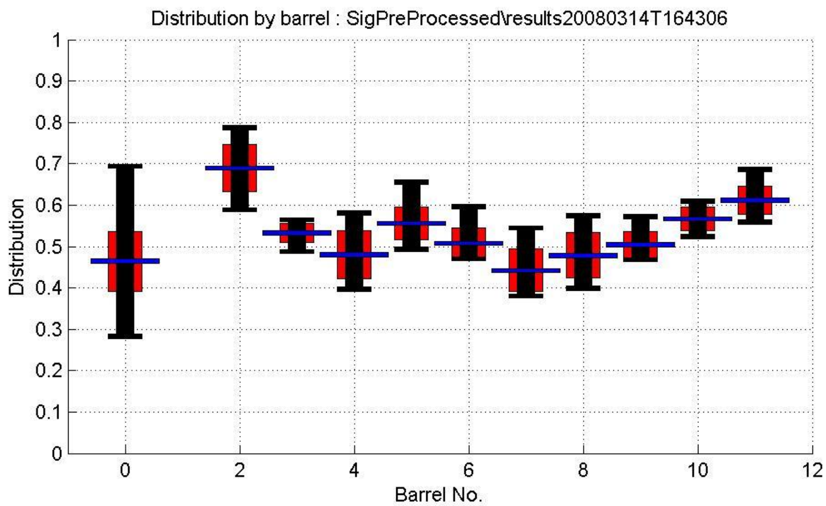

Tool : F, Toolmark LEA
Tool set 1 : 2 3 4 5 6 7 8 9 10 11, samples 6 7 8 9 10
Tool set 2 : 2 3 4 5 6 7 8 9 10 11, samples 6 7 8 9 10

	Non match	B 2	B 3	B 4	B 5	B 6	B 7	B 8	B 9	B 10	B 11
Mean	0.470	0.678	0.533	0.485	0.562	0.515	0.451	0.484	0.509	0.566	0.613
Median	0.465	0.690	0.533	0.480	0.556	0.507	0.442	0.479	0.504	0.567	0.612
Stdev	0.072	0.057	0.023	0.058	0.040	0.038	0.051	0.055	0.032	0.028	0.034
Min	0.283	0.589	0.488	0.397	0.493	0.470	0.380	0.400	0.469	0.524	0.559
Max	0.694	0.788	0.565	0.581	0.655	0.597	0.545	0.575	0.572	0.610	0.686
N	2250	20	20	20	20	20	20	20	20	20	20

xLatRes	: 2	dim	: 1
yLatRes	: 2	corrAppch	: topfivemean
XeffectiveSize	: 300	maxShiftFractionY	: 0.1
YeffectiveSize	: 1650	signalThreshold	: 0.2
Location	: centeredLeft		
topPercentage	: 3		
HPradius	: 30		
HPthreshold	: 0.99		
LPradius	: 2		
LPthreshold	: 0.1		
StatStat	: 5		
minStDecreaseRate	: 0.1		
firstOrderLevelStat	: 0		
stdTolerance	: 3		
outlierPatchX	: 70		
outlierPatchY	: 70		
maxSlope	: 60		
angularResolution	: 1		
maxAngle	: 12		
corrThresh	: 0.5		
period	: 2		
sigFilterRadius	: 2		
sigThreshold	: 0.05		
SigFilterRadius	: 100		
SigFilterThresh	: 0.99		

Figure 36: Filename F_LEA_byBarrel_20080314T164306, automated selection.

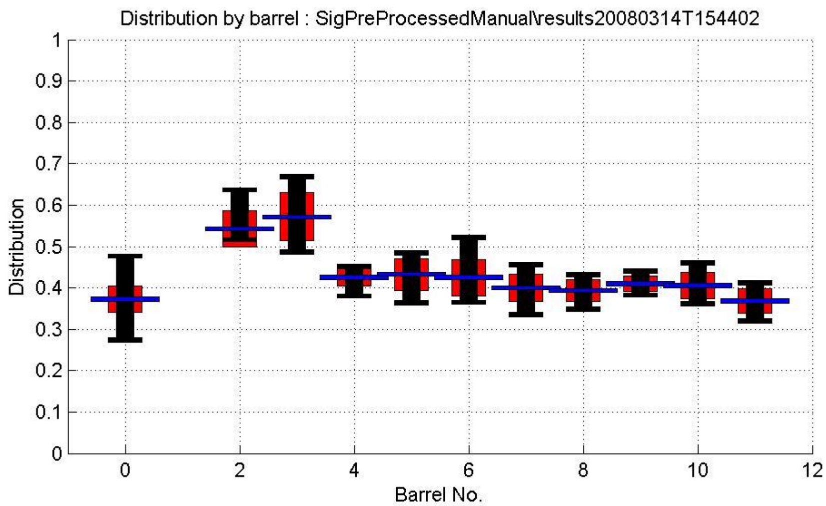

Tool : F, Toolmark LEA
Tool set 1 : 2 3 4 5 6 7 8 9 10 11, samples 6 7 8 9 10
Tool set 2 : 2 3 4 5 6 7 8 9 10 11, samples 6 7 8 9 10

	Non match	B 2	B 3	B 4	B 5	B 6	B 7	B 8	B 9	B 10	B 11
Mean	0.374	0.563	0.578	0.423	0.428	0.421	0.401	0.394	0.413	0.409	0.371
Median	0.373	0.543	0.571	0.426	0.433	0.425	0.400	0.394	0.410	0.406	0.368
Stdev	0.032	0.043	0.058	0.022	0.038	0.044	0.033	0.026	0.019	0.031	0.029
Min	0.274	0.516	0.487	0.380	0.364	0.365	0.335	0.349	0.382	0.362	0.320
Max	0.477	0.637	0.669	0.452	0.484	0.522	0.456	0.432	0.441	0.461	0.412
N	2250	20	20	20	20	20	20	20	20	20	20

xLatRes	: 2	dim	: 1
yLatRes	: 2	corrAppch	: topfivemean
XeffectiveSize	: 300	maxShiftFractionY	: 0.1
YeffectiveSize	: 1650	signalThreshold	: 0.2
Location	: centeredLeft		
topPercentage	: 3		
HPradius	: 30		
HPthreshold	: 0.99		
LPradius	: 2		
LPthreshold	: 0.1		
StatStat	: 5		
minStDecreaseRate	: 0.1		
firstOrderLevelStat	: 0		
stdTolerance	: 3		
outlierPatchX	: 70		
outlierPatchY	: 70		
maxSlope	: 60		
angularResolution	: 1		
maxAngle	: 12		
corrThresh	: 0.5		
period	: 2		
sigFilterRadius	: 2		
sigThreshold	: 0.05		
SigFilterRadius	: 100		
SigFilterThresh	: 0.99		

Figure 37: Filename F_LEA_distribution_20080314T154402, using manual region selection.

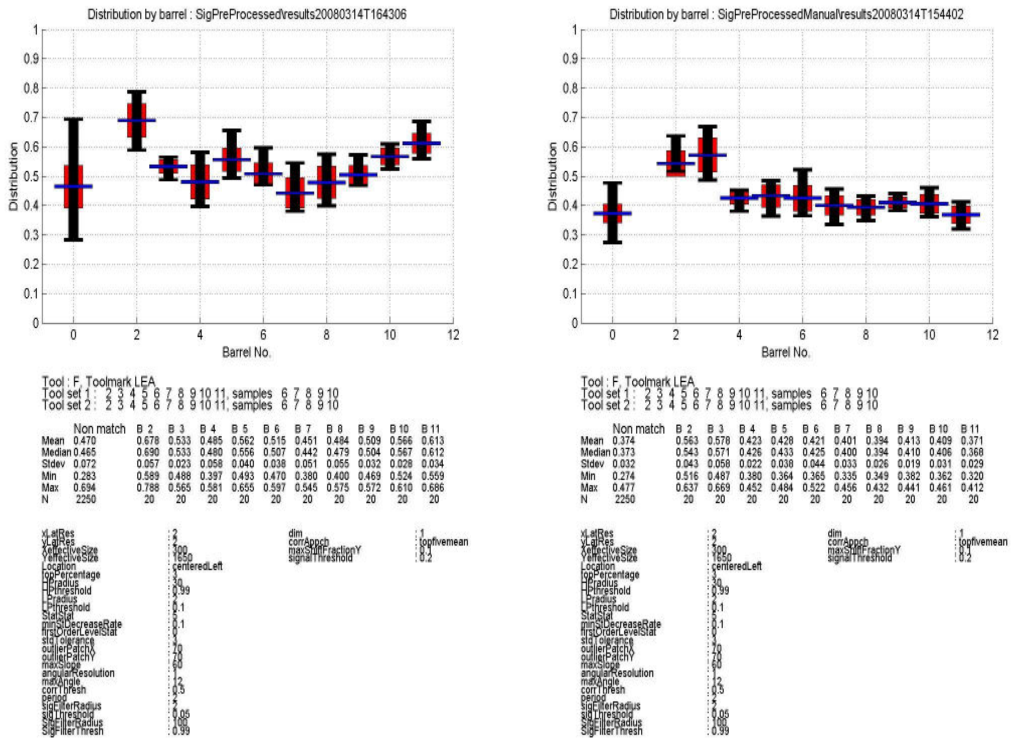

Figure 38: barrel-by-barrel automated vs. semi-manual side by side

7.4 HIPOINT

The following distributions correspond to HiPoint barrels. Figure 39 corresponds to the automated processing; no manual selection of regions of interest or striation orientations.

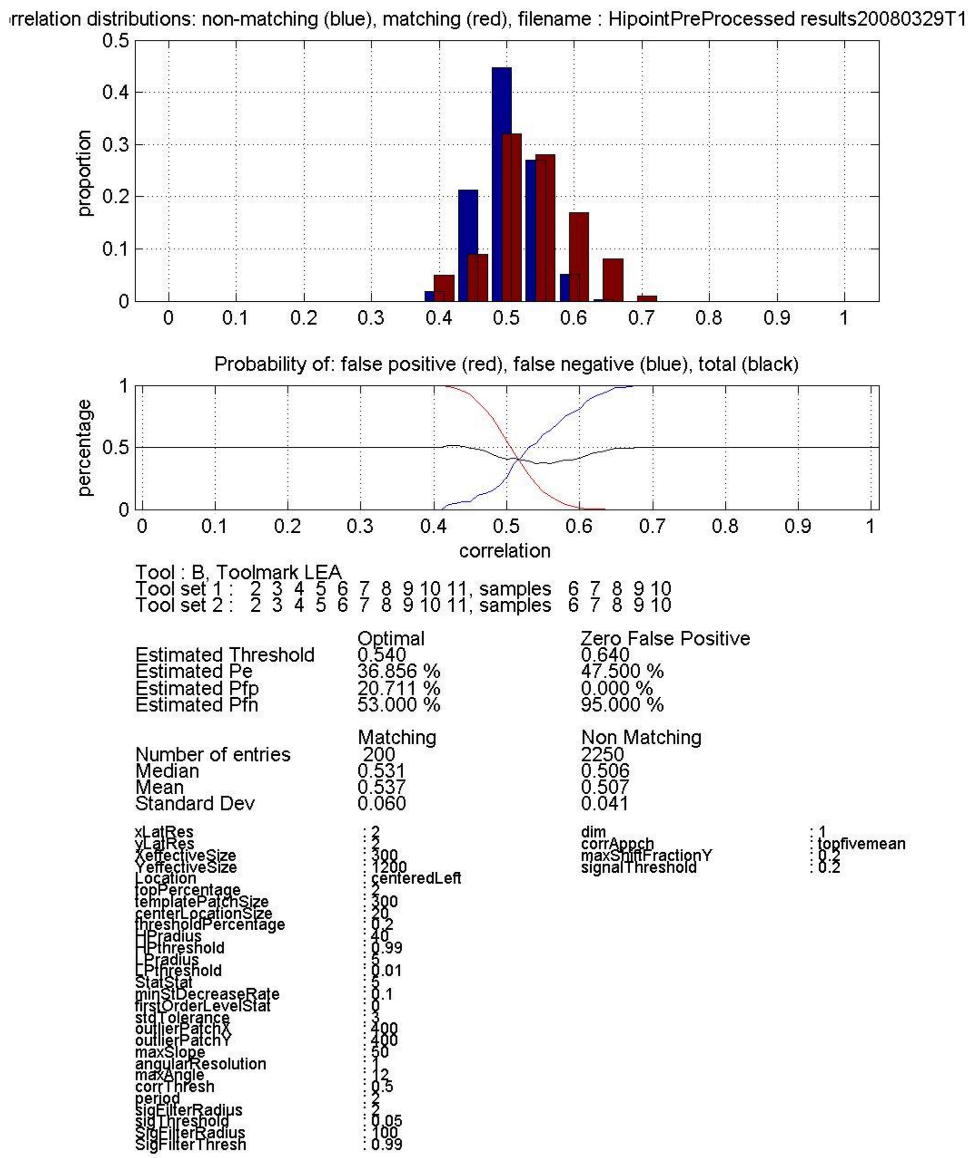

Figure 39: Filename: B_LEA_distribution_20080329T183427.jpg. automated processing

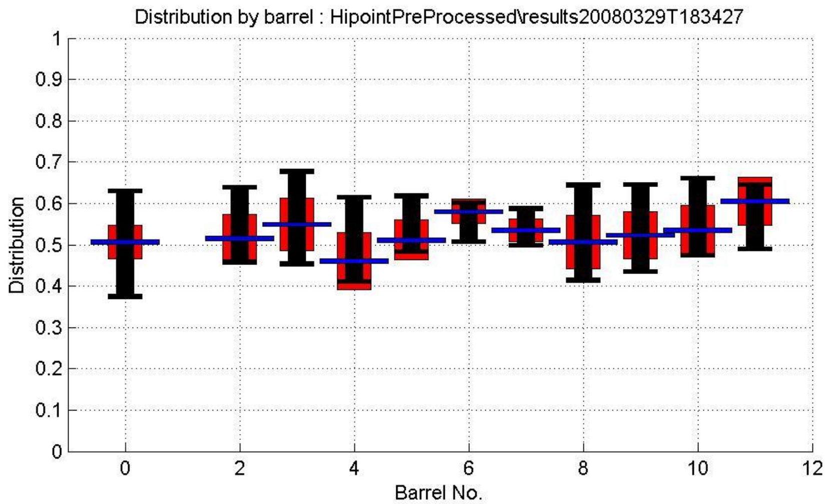

Tool : B, Toolmark LEA
Tool set 1 : 2 3 4 5 6 7 8 9 10 11, samples 6 7 8 9 10
Tool set 2 : 2 3 4 5 6 7 8 9 10 11, samples 6 7 8 9 10

	Non match	B 2	B 3	B 4	B 5	B 6	B 7	B 8	B 9	B 10	B 11
Mean	0.507	0.535	0.544	0.480	0.531	0.572	0.535	0.512	0.535	0.553	0.579
Median	0.506	0.515	0.549	0.460	0.511	0.580	0.535	0.506	0.523	0.536	0.605
Stdev	0.041	0.058	0.064	0.069	0.048	0.030	0.027	0.065	0.057	0.060	0.057
Min	0.375	0.458	0.454	0.411	0.483	0.508	0.499	0.415	0.435	0.475	0.490
Max	0.631	0.639	0.677	0.615	0.618	0.602	0.587	0.645	0.646	0.662	0.645
N	2250	20	20	20	20	20	20	20	20	20	20

xLatRes	: 2	dim	: 1
yLatRes	: 2	corrAppch	: topfivemean
XeffectiveSize	: 300	maxShiftFractionY	: 0.2
YeffectiveSize	: 1200	signalThreshold	: 0.2
Location	: centeredLeft		
topPercentage	: 2		
templatePatchSize	: 300		
centerLocationSize	: 20		
thresholdPercentage	: 0.2		
HPradius	: 40		
HPthreshold	: 0.99		
LPradius	: 5		
LPthreshold	: 0.01		
StatStat	: 5		
minStDecreaseRate	: 0.1		
firstOrderLevelStat	: 0		
stdTolerance	: 3		
outlierPatchX	: 400		
outlierPatchY	: 400		
maxSlope	: 50		
angularResolution	: 1		
maxAngle	: 12		
corrThresh	: 0.5		
period	: 2		
sigFilterRadius	: 2		
sigThreshold	: 0.05		
SigFilterRadius	: 100		
SigFilterThresh	: 0.99		

Figure 40: Filename B_LEA_byBarrel_20080329T183427.jpg, automated processing.

7.5 BRYCO

The following distributions correspond to Bryco barrels. Figure 41 corresponds to the automated processing; no manual selection of regions of interest or striation orientations.

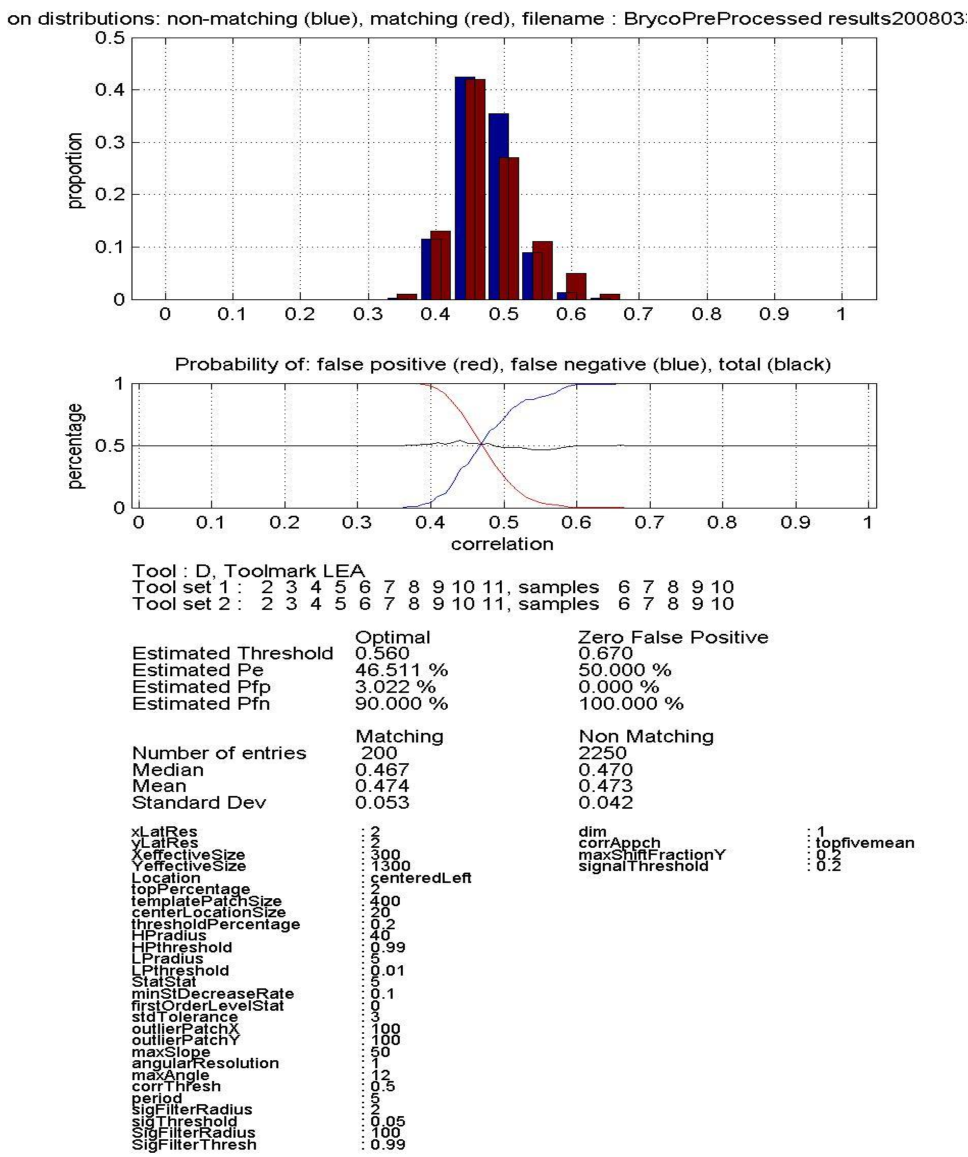

Figure 41: Filename D_LEA_distribution_20080331T050045.jpg, automated processing.

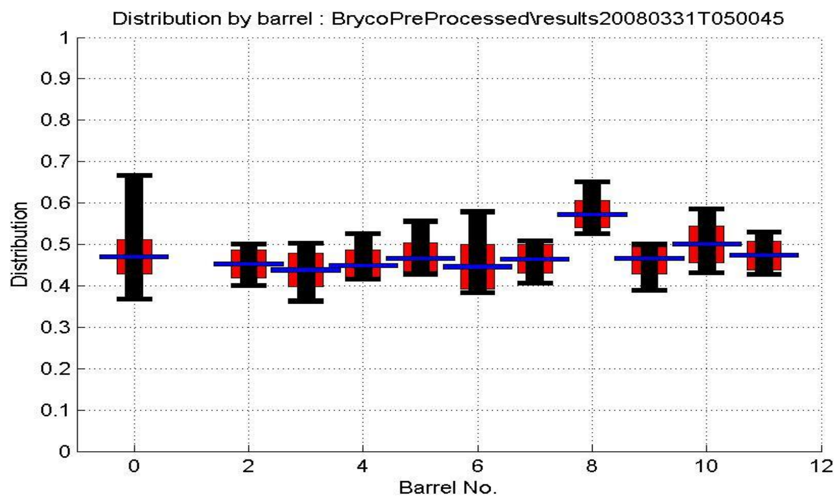

Tool : D, Toolmark LEA
Tool set 1 : 2 3 4 5 6 7 8 9 10 11, samples 6 7 8 9 10
Tool set 2 : 2 3 4 5 6 7 8 9 10 11, samples 6 7 8 9 10

	Non match	B 2	B 3	B 4	B 5	B 6	B 7	B 8	B 9	B 10	B 11
Mean	0.473	0.457	0.439	0.457	0.474	0.452	0.463	0.574	0.453	0.500	0.475
Median	0.470	0.453	0.438	0.449	0.466	0.446	0.465	0.573	0.466	0.500	0.474
Stdev	0.042	0.033	0.041	0.037	0.037	0.054	0.035	0.033	0.037	0.045	0.035
Min	0.367	0.400	0.363	0.416	0.429	0.383	0.406	0.526	0.389	0.432	0.428
Max	0.667	0.502	0.502	0.526	0.556	0.579	0.509	0.651	0.500	0.585	0.529
N	2250	20	20	20	20	20	20	20	20	20	20

xLatRes	: 2	dim	: 1
yLatRes	: 2	corrAppch	: topfivemean
XeffectiveSize	: 300	maxShiftFractionY	: 0.2
YeffectiveSize	: 1300	signalThreshold	: 0.2
Location	: centeredLeft		
topPercentage	: 2		
templatePatchSize	: 400		
centerLocationSize	: 20		
thresholdPercentage	: 0.2		
HPradius	: 40		
HPthreshold	: 0.99		
LPradius	: 5		
LPthreshold	: 0.01		
StatStat	: 5		
minStDecreaseRate	: 0.1		
firstOrderLevelStat	: 0		
stdTolerance	: 3		
outlierPatchX	: 100		
outlierPatchY	: 100		
maxSlope	: 50		
angularResolution	: 1		
maxAngle	: 12		
corrThresh	: 0.5		
period	: 5		
sigFilterRadius	: 2		
sigThreshold	: 0.05		
SigFilterRadius	: 100		
SigFilterThresh	: 0.99		

Figure 42: Filename D_LEA_byBarrel_20080331T050045.jpg, automated processing.

7.6 Summary Comparison of Results

	Browning, Winchester									
	matching				non-matching				Pe, 5 LEA mean	
	N	mean	median	std	N	mean	median	std	min	zero fp
2005 Study	450	0.552	0.555	0.095	4500	0.446	0.450	0.054	18.1%	36.2%
New Study (MuSur	200	0.542	0.537	0.101	2250	0.368	0.366	0.028	6.4%	17.5%
New Study, Manua	200	0.582	0.584	0.092	2250	0.365	0.363	0.030	3.0%	13.0%

	SIG, Winchester									
	matching				non-matching				Pe, 5 LEA	
	N	mean	median	std	N	mean	median	std	min	zero fp
2005 Study	441	0.504	0.500	0.046	4410	0.493	0.491	0.045	45.2%	50.0%
New Study (MuSur	200	0.539	0.542	0.077	2250	0.470	0.465	0.072	31.2%	48.5%
New Study, Manua	200	0.440	0.418	0.076	2250	0.374	0.373	0.032	25.7%	38.5%

	Taurus, Winchester									
	matching				non-matching				Pe, 5 LEA	
	N	mean	median	std	N	mean	median	std	min	zero fp
2005 Study	225	0.572	0.578	0.066	1000	0.471	0.468	0.039	17.6%	39.3%
New Study (MuSur	100	0.589	0.585	0.078	500	0.443	0.439	0.026	6.8%	15.0%
New Study, Manua	100	0.562	0.562	0.081	500	0.421	0.420	0.025	7.6%	10.0%

	HiPoint, Winchester									
	matching				non-matching				Pe, 5 LEA	
	N	mean	median	std	N	mean	median	std	min	zero fp
2005 Study	450	0.481	0.474	0.053	4500	0.449	0.450	0.039	36.3%	49.1%
New Study (MuSur	200	0.537	0.531	0.060	2250	0.507	0.506	0.041	36.9%	47.5%
New Study, Manual (MuSurf)										

	Bryco, Winchester									
	matching				non-matching				Pe, 5 LEA	
	N	mean	median	std	N	mean	median	std	min	zero fp
2005 Study	450	0.456	0.461	0.087	4500	0.451	0.458	0.084	47.1%	49.9%
New Study (MuSur	200	0.474	0.467	0.053	2250	0.473	0.470	0.042	46.5%	50.0%
New Study, Manual (MuSurf)										